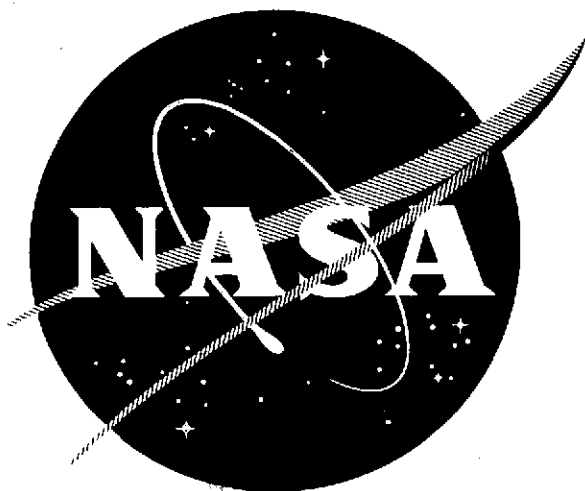


2mif



NASA CR-134522
WANL-M-FR-73-005

FINAL REPORT
DEVELOPMENT OF DUCTILE HIGH-STRENGTH
CHROMIUM ALLOYS
PHASE II

BY
A. M. FILIPPI



WESTINGHOUSE ASTRONUCLEAR LABORATORY

(NASA-CR-134522) DEVELOPMENT OF DUCTILE
HIGH-STRENGTH CHROMIUM ALLOYS, PHASE 2
Final Report (Westinghouse Astronuclear
Lab., Pittsburgh) 78 p HC \$6.00
80
N74-13245
Unclas
24604
CSCL 11F G3/17

prepared for
NATIONAL AERONAUTICS AND SPACE ADMINISTRATION

NASA LEWIS RESEARCH CENTER
CONTRACT NAS 3-15559

NOTICE

This report was prepared as an account of Government-sponsored work. Neither the United States, nor the National Aeronautics and Space Administration (NASA), nor any person acting on behalf of NASA:

- A.) Makes any warranty or representation, expressed or implied, with respect to the accuracy, completeness, or usefulness of the information contained in this report, or that the use of any information, apparatus, method, or process disclosed in this report may not infringe privately-owned rights; or
- B.) Assumes any liabilities with respect to the use of, or for damages resulting from the use of, any information, apparatus, method or process disclosed in this report.

As used above, "person acting on behalf of NASA" includes any employee or contractor of NASA, or employee of such contractor, to the extent that such employee or contractor of NASA or employee of such contractor prepares, disseminates, or provides access to any information pursuant to his employment or contract with NASA, or his employment with such contractor.

Requests for copies of this report should be referred to

National Aeronautics and Space Administration
Scientific and Technical Information Facility
P. O. Box 33
College Park, Maryland 20740

1. Report No. NASA CR-134522		2. Government Accession No.		3. Recipient's Catalog No.	
4. Title and Subtitle Development of Ductile High-Strength Chromium Alloys - Phase II				5. Report Date September, 1973	
				6. Performing Organization Code	
7. Author(s) A. M. Filippi				8. Performing Organization Report No. WANL-M-FR-73-005	
				10. Work Unit No.	
9. Performing Organization Name and Address Westinghouse Astronuclear Laboratory P. O. Box 10864 Pittsburgh, Pa. 15236				11. Contract or Grant No. NAS 3-15559	
				13. Type of Report and Period Covered Contractor Report	
12. Sponsoring Agency Name and Address National Aeronautics and Space Administration Washington, D. C. 20546				14. Sponsoring Agency Code	
15. Supplementary Notes Project Manager, William D. Klopp, NASA Lewis Research Center, Cleveland, Ohio					
16. Abstract Strength and ductility were evaluated for chromium alloys dispersion hardened with the putative TaC, TaB, CbC, and CbB compounds. TaC and TaB proved to be the most potent strengtheners, but when combined, their effect far outweighed that produced individually. Tests at 1422°K (2100°F) on an alloy containing these two compounds at the combined level of 0.5 m/o revealed a 495 MN/m ² (70 ksi) tensile strength for wrought material, and a 100 hour rupture strength of 208 MN/m ² (30 ksi) when solution annealed and aged to maximize creep resistance. These levels of high temperature strength greatly exceed that reported for any other chromium-base alloy. The ductile-to-brittle transition temperature (DBTT) of the two phase strengthened alloy occurred at ~588°K (600°F) when heat treated to optimize creep strength and was not improved by fabrication to produce a wrought and recovered microstructure. The lowest DBTT measured on any of the alloys investigated was 422°K (300°F). Strengthening phases actually formed in Cr-Ta-B and Cr-Cb-B compositions are probable M ₂ CrB ₂ (M = Ta or Cb) compounds of tetragonal crystal structure; a = 5.9 x 10 ⁻¹⁰ m (5.9 Å), c = 3.2 x 10 ⁻¹⁰ m (3.2 Å). The likely habit relationship between these compounds and chromium is postulated. Cube habit coherency was identified for TaC precipitation in chromium by electron microscopy. In another study, the maximum solubility of carbon in chromium was indicated to lie between 3/4 and 1 a/o and that of boron to be < 1/2 a/o.					
17. Key Words (Suggested by Author(s)) TaB and TaC Strengthened Mechanical Properties Composition Effects Phase Stability Solubility				18. Distribution Statement UNCLASSIFIED - UNLIMITED	
19. Security Classif. (of this report) UNCLASSIFIED		20. Security Classif. (of this page) UNCLASSIFIED		21. No. of Pages 7	22. Price* \$3.00

* For sale by the National Technical Information Service, Springfield, Virginia 22151

FOREWORD

The work described herein was performed at the Astronuclear Laboratory, Westinghouse Electric Corporation, under NASA Contract NAS 3-15559. Mr. W. D. Klopp, NASA-Lewis Research Center, served as Project Manager.

TABLE OF CONTENTS

	<u>Title</u>	<u>Page No.</u>
1.0	SUMMARY	1
2.0	INTRODUCTION	4
3.0	MATERIALS AND EXPERIMENTAL PROCEDURES	6
3.1	Alloy Constituents	6
3.2	Melting, Fabrication, and Evaluation	6
4.0	EXPERIMENTAL PROGRAM AND DISCUSSION	8
4.1	Properties of Carbide and Boride Strengthened Alloys	8
4.1.1	Ingot Analysis	8
4.1.2	Fabrication	8
4.1.3	Optical Microstructure	12
4.1.4	Tensile Properties at 1422°K (2100°F)	24
4.1.5	Creep Properties at 1422°K (2100°F)	27
4.1.6	Ductile-to-Brittle Transition Behavior	37
4.1.7	Precipitation of the Strengthening Phases	37
4.1.8	Oxidation Behavior of 1422°K (2100°F)	42
4.2	Influence of Thermomechanical Processing on the Properties of Cr-.50Ta(C, B)	45
4.2.1	Fabrication	45
4.2.2	Optical Microstructure	47
4.2.3	Tensile and Creep Properties at 1422°K (2100°F)	50
4.2.4	Ductile-to-Brittle Transition Behavior	52
4.3	Solubility of Carbon and Boron in Chromium	55
4.3.1	Chemical Analysis	55
4.3.2	Solubility Data	55

TABLE OF CONTENTS (Continued)

	<u>Title</u>	<u>Page No.</u>
4.4	Identification of Borides Formed in Cr-Ta-B and Cr-Cb-B Alloys	64
4.4.1	Previously Reported Data	64
4.4.2	Current Program	65
5.0	CONCLUSIONS	70
6.0	REFERENCES	71

LIST OF ILLUSTRATIONS

	<u>Title</u>	<u>Page No.</u>
1	The Relationship Between Oxygen Contamination and Residual Yttrium Content in Experimental Heats	10
2	The Influence Heat Treatment for 1 hour at 1589 to 1839°K (2400 to 2850°F) has on the Microstructure of the Cr-.50Ta(C,B) Alloy	14
3	The Influence Heat Treatment for 1 hour at 1589 to 1839°K (2400 to 2850°F) has on the Microstructure of the Cr-.5TaC Alloy	15
4	The Influence Heat Treatment for 1 hour at 1589 to 1839°K (2400 to 2850°F) has on the Microstructure of the Cr-.75TaC Alloy	16
5	The Influence Heat Treatment for 1 hour at 1589 to 1839°K (2400 to 2850°F) has on the Microstructure of the Cr-1.00TaC Alloy	17
6	The Influence Heat Treatment for 1 hour at 1589 to 1839°K (2400 to 2850°F) has on the Microstructure of the Cr-.75CbC Alloy	18
7	The Influence Heat Treatment for 1 hour at 1589 to 1839°K (2400 to 2850°F) has on the Microstructure of the Cr-.5TaB Alloy	19
8	The Influence Heat Treatment for 1 hour at 1589 to 1839°K (2400 to 2850°F) has on the Microstructure of the Cr-.75TaB Alloy	20
9	The Influence Heat Treatment for 1 hour at 1589 to 1839°K (2400 to 2850°F) has on the Microstructure of the Cr-1.00TaB Alloy	21
10	The Influence Heat Treatment for 1 hour at 1589 to 1839°K (2400 to 2850°F) has on the Microstructure of the Cr-.75CbB Alloy	22
11	The Influence of Heat Treatment on Hardness of the Carbide and Boride Strengthened Alloys	23
12	The Influence of Test Stress on the Creep Rates Observed at 1422°K (2100°F) for the Four Most Creep Resistant Experimental Compositions	32
13	The Influence of Test Stress on the Rupture Times Observed at 1422°K (2100°F) for the Four Most Creep Resistant Experimental Compositions	33
14	A Larson-Miller Comparison of Rupture Strengths of the Most Superior Superalloys and Experimental Chromium-base Compositions	36
15	The Influence of Test Temperature on Tensile Reduction of Area Observed on the Carbide and Boride Strengthened Alloys	39

LIST OF ILLUSTRATIONS (Continued)

	<u>Title</u>	<u>Page No.</u>
16	The Unit Cells and Lattice Dimensions of Chromium and the M_2CrB_2 and MC Phases	41
17	TaC Precipitation in the Cr-0.50TaC Alloy Solution Annealed then Aged 3 Hours at 1422°K (2100°F) (110) Foil Orientation	43
18	An Outline of the Thermomechanical Processing Study	46
19	The Microstructure of Piece 26A in the As-extruded Condition	48
20	The Influence of Heat Treatment on Microstructure and Hardness of the Cr-.50Ta(C,B) Alloy Fabricated by Three Different Processes	49
21	The Influence of Fabrication History on the Ductile-to-Brittle Transition Behavior of Cr-.50Ta(C,B)	54
22	The Influence of Heat Treatment on Grain Size of the Cr-C and Cr-B Compositions	57
23	Microstructural Response of the Cr-0.75C Composition to Heat Treatment	58
24	Overall Grain Boundary Liquation Caused in the Cr-1.0C Composition by Heat Treatment at 1822°K (2820°F)	60
25	Microstructural Response of the Cr-0.5B Composition to Heat Treatment	61
26	Terminal Solubility and Melting in the Cr-C System	62
27	Terminal Solubility and Melting in the Cr-B System	63
28	Diffraction Patterns of Boride Phases Extracted from Tantalum and Columbium Boride Strengthened Chromium-base Alloys	66

LIST OF TABLES

	<u>Title</u>	<u>Page No.</u>
1	Chemical Analyses of the Carbide and Boride Strengthened Alloys	9
2	Effect of Processing on Hardness of the Carbide and Boride Strengthened Alloys	11
3	Tensile Properties of the Carbide and Boride Strengthened Alloys Determined at 1422°K (2100°F)	25
4	Creep Behavior of the Carbide and Boride Strengthened Alloys Determined at 1422°K (2100°F)	28
5	A Comparison of the Stress Dependency Parameters Displayed by the Four Highest Creep Strength Alloys	35
6	Low Temperature Tensile Properties of the Carbide and Boride Strengthened Alloys Heat Treated for Optimum Stress-Rupture Strength	38
8	The Influence of Fabrication History on Tensile and Creep Properties of the Cr-. 50Ta(C, B) Alloy Measured at 1422°K (2100°F)	51
9	The Influence of Fabrication History on Low Temperature Tensile Properties of Cr-. 50Ta(C, B)	53
10	Chemical Analyses of the Solubility Study Alloys	56
11	Indexed Diffraction Data for the Tantalum-rich X Phase Boride and that Reported for a Mixed Metal Boride of M_3B_2 Type	67
12	Indexed Diffraction Data for the Columbium-rich X Phase Boride	69

1.0 SUMMARY

Elevated temperature tensile and creep strength and ductile-to-brittle transition behavior were evaluated for chromium alloys dispersion hardened with the putative TaC, TaB, CbC, and CbB compounds. Alloying contents investigated were: 0.50, 0.75, and 1.00 TaC (m/o); 0.50, 0.75, and 1.00 TaB; 0.75 CbC; 0.75 CbB; and 0.25 TaC + 0.25 TaB*. The experimental compositions were prepared by induction melting and fabricated to test rod at 1422°K (2100°F). Fabrication left each alloy with a wrought (worked) microstructure. In this condition, measurement of high temperature tensile strength for alloys containing a single boride or carbide revealed a relationship to the chemistry of these phases but not to the amount present. The arrangement of individual strengthening phases in increasing order of potency was: CbC, TaC, CbB, and TaB. Tensile strengths at 1422°K (2100°F) ranged from approximately 173 MN/m² (25 ksi) for Cr-.75CbC to 346 MN/m² (50 ksi) for the Cr-TaB alloys. The highest wrought material tensile strength, however, was measured on the composition containing TaC and TaB combined to the 0.5 m/o level; 485 MN/m² at 1422°K (70 ksi at 2100°F). In the solution annealed and aged condition, a heat treatment found necessary to maximize creep strength, lowest to highest tensile strengths spanned 173 to 250 MN/m² at 1422°K (25 to 36 ksi at 2100°F), but the order of strength arrangement remained roughly as noted for the wrought alloys.

None of the wrought alloys displayed an outstanding creep strength. All were tested at 1422°K and 104 MN/m² (2100°F and 15 ksi), and ruptured in the time period of a day or less. Solutioning and aging treatments, however, improved the creep strength of every alloy. This involved a 15 minute heat treatment at 1811 or 1839°K (2800 or 2850°F) followed by a three hour age at 1422°K (2100°F).

Highest creep strengths in the solution annealed and aged condition were measured on Cr-.75TaC, Cr-1.00TaC, Cr-.50TaB, and Cr-.50Ta(C,B). The stresses to cause failure in 100 hours at 1422°K (2100°F) for the 0.75TaC, 1.00TaC, and 0.50TaB strengthened compositions were,

* Given as 0.50Ta(C,B) in composition notations.

respectively, 132, 111, and 125 MN/m² (19, 16, and 18 ksi). By comparison, this stress level for the Cr-.50Ta(C,B) alloy was 208 MN/m² (30 ksi). A creep strength of this magnitude far exceeds that reported for any chromium-base alloy. When combined, the individual strengthening potentials of TaC and TaB must act additively or possibly even synergistically.

The stress dependency of creep was also evaluated for the four strongest experimental alloys in their optimum condition. Values of the stress exponent ranging from 3 to 5 were obtained for the Cr-.50TaB and Cr-.50Ta (C,B) compositions. The magnitudes of this factor were 7 and 13, respectively, for Cr-.75TaC and Cr-1.00TaC. Alloying content appears to control the stress dependency of creep.

Ductile-to-brittle transition temperatures (DBTT) were determined for each alloy in the solution annealed and aged condition. The lowest DBTT observed for any alloy was 422°K (300°F) and the highest was 644°K (700°F). Attempts at lowering the DBTT of the high strength Cr-.50Ta (C, B) alloy by fabrication to produce a wrought and recovered microstructure were successful.

Diffraction patterns obtained from the unknown tantalum and columbium-rich strengthening phases actually formed in Cr-Ta-B and Cr-Cb-B alloys were successfully indexed in the tetragonal system. The indexed results were also linked to similar data reported for a complex mixed metal boride and concluded to possibly be compounds of Ta₂CrB₂ and Cb₂CrB₂ stoichiometry. Calculated lattice parameters are: $a = 5.905 \times 10^{-10} \text{ m (5.905 \AA)}$, $c = 3.231 \times 10^{-10} \text{ m (3.231 \AA)}$ for Ta₂CrB₂; $a = 5.925 \times 10^{-10} \text{ m (5.925 \AA)}$, $c = 3.240 \times 10^{-10} \text{ m (3.240 \AA)}$ for Cb₂CrB₂. The likely habit relationship between these compounds and chromium is postulated as: $\langle 100 \rangle \text{ Cr} // \langle 100 \rangle \text{ M}_2\text{CrB}_2$, $\langle 110 \rangle \text{ Cr} // \langle 110 \rangle \text{ M}_2\text{CrB}_2$; $\{100\} \text{ Cr} // \{100\} \text{ M}_2\text{CrB}_2$. The cube habit coherency relationship was identified by electron microscopy for the precipitation of TaC in chromium, i.e., $\langle 110 \rangle \text{ Cr} // \langle 100 \rangle \text{ TaC}$, $\langle 100 \rangle \text{ Cr} // \langle 110 \rangle \text{ TaC}$ $\{100\} \text{ Cr} // \{100\} \text{ TaC}$.

A study of carbon and boron solubility in chromium was also made. Samples of binary heats spanning 0.5 to 1.0 a/o carbon and boron contents were annealed at successively higher temperatures and metallographically examined for evidence of solutioning, assumed to be indicated by the occurrence of exaggerated grain growth. The maximum solubility of carbon in chromium was indicated to lie between 3/4 and 1 a/o and that of boron to be $<1/2$ a/o.

2.0 INTRODUCTION

The ductile-to-brittle transition temperature of chromium is generally increased by strength enhancing solute additions in proportion to the amount present⁽¹⁻³⁾. To minimize this effect, current efforts at strength improvement have emphasized the investigation of dilute dispersion hardened compositions. Early work by Ryan demonstrated that chromium could be dispersion strengthened without serious sacrifice of low temperature ductility by using carbides of the groups IVB and VB metals⁽⁴⁾. On more recent work sponsored by NASA, Filippi evaluated the dispersion strengthening potential of both carbides and borides of these metals^(5,6). Emphasis was placed on alloys containing 0.5 m/o of the compounds. The tantalum phases were found to exert the most potent strengthening effect, and those of columbium were second best in this respect. This result formed the basis for the present work.

Nine experimental chromium-base compositions given below were studied on an alloy development task. How properties are influenced by TaC and TaB content was examined by preparing alloys containing 0.50, 0.75, and 1.00 m/o of these compounds. A complex composition, Cr-.50Ta(C,B), was evaluated to obtain a data comparison with solely carbide or boride strengthened materials. The investigation of CbC and CbB strengthened compositions allowed the relative merits of these phases to be compared with the TaC and TaB compounds at a level of 0.75 m/o. Ingots of each composition were induction melted and fabricated to test rod by extrusion and swaging at 1422°K (2100°F). Evaluation involved the measurement of characteristics important to jet engine applications, e. g. elevated temperature tensile and creep properties, ductile-to-brittle transition behavior, microstructure stability, oxidation behavior.

A thermomechanical processing experiment formed another investigation. This comprised a study of how annealing, extrusion, and swaging temperature variations influenced strength and ductility of the Cr-.50Ta(C,B) alloy.

The examination of carbon and boron solubility in chromium and identification of precipitates formed in the boride strengthened alloys were other studies undertaken. The latter project involved an in-depth analysis of x-ray diffraction patterns obtained on borides extracted from Cr-TaB and Cr-CbB alloys. Binary heats spanning 0.5 to 1.0 a/o carbon and boron contents were prepared and examined on the solubility study. Evaluation involved isochronal anneals at successively higher temperatures until solutioning was indicated by the occurrence of exaggerated grain growth.

Experimental Alloys, m/o

Cr-.50TaC
 Cr-.75TaC
 Cr-1.00TaC
 Cr-.50TaB*
 Cr-.75TaB*
 Cr-1.00TaB
 Cr-.50Ta(C,B)*** (.50 a/o Ta, .25 a/o C, .25 a/o B)
 Cr-.75CbC
 Cr-.75CbB**

*,** Ta_2CrB_2 and Cb_2CrB_2 are the approximate formulas of the strengthening borides actually formed in these alloys. For simplicity they are referred to as TaB and CbB in composition notations.

*** Both Ta_2CrB_2 and TaC form in this alloy.

3.0 MATERIALS AND EXPERIMENTAL PROCEDURES

3.1 ALLOY CONSTITUENTS

Electrolytic chromium was used as the base for the experimental carbide and boride strengthened alloys. Contaminant levels in this material were typically: 150 ppm oxygen (by weight), 20-40 ppm nitrogen, carbon ≤ 40 ppm, other common impurities each ≤ 20 ppm. Alloying additions were of commercial purity. This purity level was considered adequate since compositions studied contained 2 a/o or less total alloying additions; as a consequence, their intrinsic impurity content was dominated by that present in the chromium base material.

Extremely high purity chromium prepared by the iodide process was used as the base for the solubility study alloys. Contaminant levels in this material were: 15 ppm oxygen, 3 ppm nitrogen, 7 ppm carbon, other common impurities ≤ 10 ppm.

3.2 MELTING, FABRICATION, AND EVALUATION

Brief descriptions of the melting, fabrication, and evaluation techniques are given below. These procedures are thoroughly covered in References 6 and 7.

The carbide and boride strengthened alloys were prepared as 4.5 kg (10 pounds) induction melted heats. The following were steps taken to avoid serious oxygen contamination and solidification cracks:

1. Charges were premelted and homogenized by the nonconsumable arc technique thereby minimizing the induction melting time.
2. The zirconia induction melt crucible and associated ceramic parts were heated under vacuum prior to introducing a charge to drive off adsorbed contaminants.
3. Each heat was scavenged by a 0.3 a/o yttrium addition.
4. Ingots were cast into zirconia lined molds to lessen the solidification rate.

The induction melted ingots were fabricated into 0.95 cm (.375 in.) test rod by extrusion and swaging. This involved hermetic encasement in steel* followed by an 85% extrusion reduction and a 75% swaging reduction. The total ingot-to-rod deformation was 96%. All fabrication on the nine ingots prepared for the alloy development task was accomplished at 1422°K (2100°F). Fabrication temperatures were varied on the thermomechanical processing study.

The binary Cr-C and Cr-B solubility study compositions were prepared as 0.25 kg nonconsumable arc melted ingots. They were encased in steel picture frames and reduced 75% to 0.2 cm (0.08 in.) sheet by rolling at 1310°K (1900°F).

Tensile and creep data were obtained using a specimen of 2.54 cm (1 inch) gage length and 0.45 cm (3/16 in.) gage diameter. Tests to determine tensile ductile-to-brittle transition temperatures** were run in air at a 0.05 cm/min (0.02 inch/minute) crossheat rate. The samples were electropolished in solution of 7 parts methanol and 1 part sulfuric acid prior to testing. Creep and tensile tests at 1422°K (2100°F) were conducted in a cold wall tantalum resistance heated unit under vacuum of $6.5 \times 10^{-4} \text{ N/m}^2$ (5×10^{-6} torr). A crosshead rate of 0.13 cm/min (0.05 inch/minute) was used on the 1422°K (2100°F) tensile tests.

Heat treatments were performed under vacuum of $6.5 \times 10^{-4} \text{ N/m}^2$ (5×10^{-6} torr) and concluded by a helium quench. Specimen preparation for examination by optical microscopy involved standard techniques with microstructure revealed by electrolytic etching in a 5% solution of chromic acid in water. Carbide and boride phase identification involved extraction in a 10% bromine-methanol solution and examination by standard Debye powder pattern x-ray diffraction techniques. Oxidation tests were run in air on a continuous weight recording thermobalance at 1422°K (2100°F). The test coupons measured ~1.3 cm diameter x 0.4 cm thick (~0.5 in. dia. x 0.15 in. thk.). They were prepared for testing by surface finishing on 600 grit SiC paper followed by ultrasonic cleaning in methanol.

* A portion of one ingot extruded on the thermomechanical processing study at 1811°K (2800°F) was canned in molybdenum.

** Referred to in the text as DBTT.

4.0 EXPERIMENTAL PROGRAM AND DISCUSSION

The results of tests and data analyses are presented in this section. Distinguishable projects comprise four units of discussion and are entitled: 1. Properties of Carbide and Boride Strengthened Alloys; 2. Influence of Thermomechanical Processing on the Properties of Cr-.50Ta(C,B); 3. Solubility of C and B in Chromium; and 4. Identification of Borides Formed in Cr-Ta-B and Cr-Cb-B Compositions. Some general information reported on the first project includes data on material prepared for the thermomechanical processing study.

4.1 PROPERTIES OF CARBIDE AND BORIDE STRENGTHENED ALLOYS

4.1.1 Ingot Analyses

The results of chemical analyses for alloying elements and impurities are presented in Table 1. Nominal compositions were closely approached on each study alloy. Retained yttrium levels varied greatly, however, ranging from below 0.01 to 0.18 a/o. The Cr-.50TaC composition, in which <0.01 a/o yttrium was retained, was most severely contaminated with oxygen and contained 0.15 a/o of the element. The oxygen level of material containing 0.18 a/o yttrium was lower by two orders of magnitude. An inverse relationship between yttrium and oxygen contents was generally observed, a point graphically illustrated in Figure 1. Nitrogen contamination was not severe in any alloy. The highest level of this contaminant was 0.024 a/o.

4.1.2 Fabrication

Ingot to test material conversion involved reductions of 85% by extrusion then 75% by swaging. Hardness of the ingots and changes caused by fabrication are reported in Table 2. Fabrication of heats 16 through 25 was accomplished entirely at 1422°K (2100°F) and without exception caused hardness to increase above the as-cast level. The highest hardness levels were obtained on Ta(C,B) and TaB strengthened compositions, ~250 - 270 DPH. Hardness of other alloys fell in the range of ~190 to 220 DPH. Microstructural examination of as-fabricated material revealed heavily deformed microstructures typical of cold worked material.

Table 1. Chemical Analyses of the Carbide and Boride Strengthened Alloys

Induction Melt No.	Nominal Composition (m/o)	Analyzed Composition (a/o)*						
		Ta	Cb	C	B	Y	O	N
16	Cr-.50Ta(C,B)	.52	--	.33	.25	.18	.006	.024
18	Cr-.50TaC	.56	--	.57	--	<.01	.150	.005
19	Cr-.75TaC	.78	--	.77	--	.03	.101	.009
20	Cr-1.00TaC	1.02	--	1.14	--	.17	.009	.008
21	Cr-.75CbC	--	.81	.85	--	.18	.009	.006
22	Cr-.50TaB	.54	--	--	.49	.12	.040	.009
23	Cr-.75TaB	.83	--	--	.69	.10	.046	.008
24	Cr-1.00TaB	1.06	--	--	.99	.11	.077	.008
25	Cr-.75CbB	--	.80	--	.74	.15	.022	.008
26**	Cr-.50Ta(C,B)	.52	--	.23	.20	.11	.023	.003
27**	Cr-.50Ta(C,B)	.53	--	.23	.20	.07	.024	.002

* Yttrium analysis obtained on extruded material. Other results are ingot top analysis.

** Prepared for the TMP study.

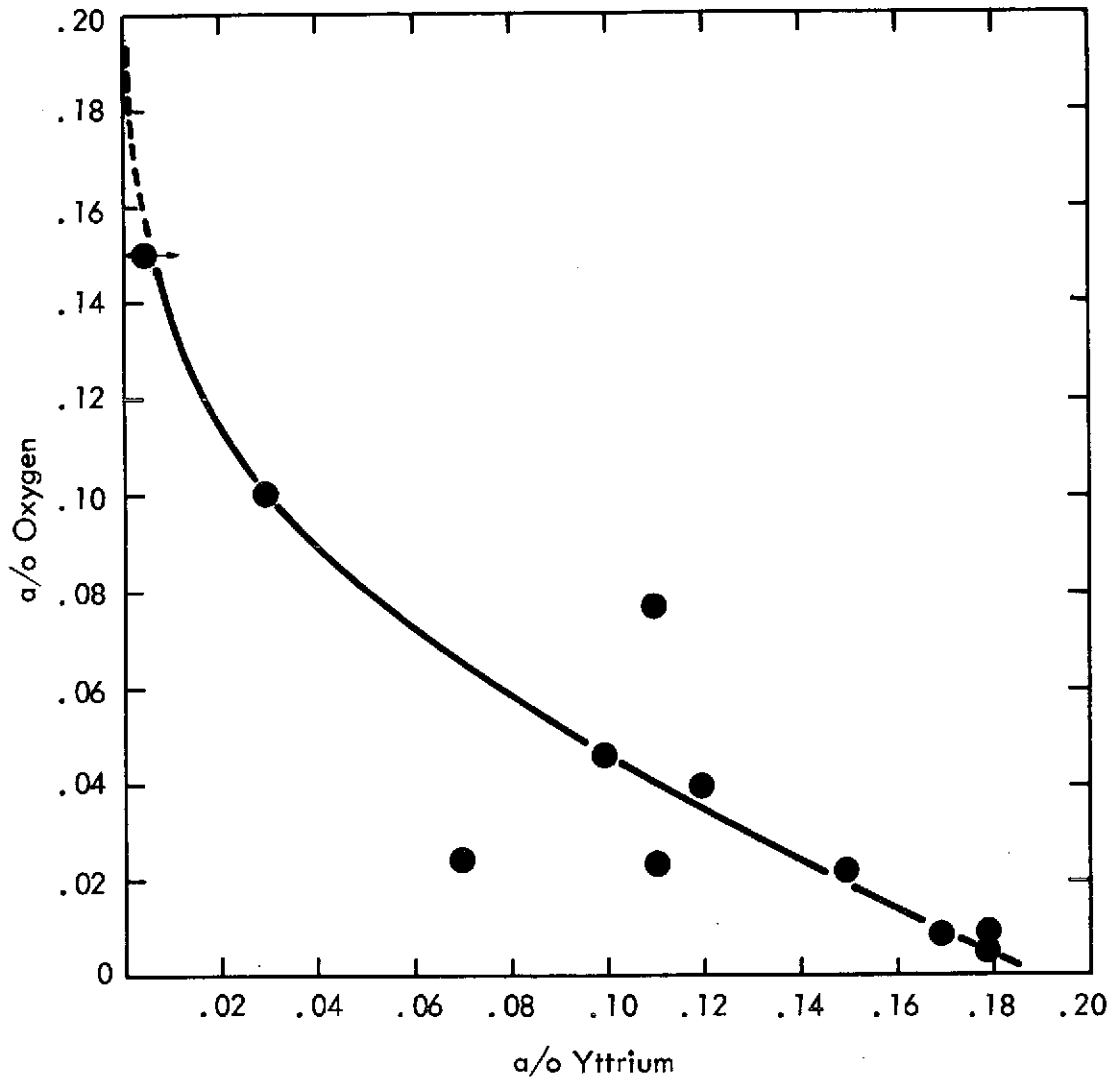


Figure 1. The Relationship Between Oxygen Contamination and Residual Yttrium Content in Experimental Heats. (Data presented in Table 1)

Table 2. Effect of Processing on Hardness of the Carbide and Boride Strengthened Alloys*

Induction Melt No.	Nominal Composition m/o	Diamond Pyramid Hardness; 30 kg Load		
		Cast	Extruded	Swaged
16	Cr-.50Ta(C, B)	168	235	271
18	Cr-.50TaC	165	224	219
19	Cr-.75TaC	170	207	188
20	Cr-1.00TaC	170	222	211
21	Cr-.75CbC	158	203	202
22	Cr-.50TaB	177	230	264
23	Cr-.75TaB	200	249	250
24	Cr-1.00TaB	205	274	250
25	Cr-.75CbB	184	233	217
26**	Cr-.50Ta(C, B)	170	177, pt. (a) 234, pt. (b)	248 263
27**	Cr-.50Ta(C, B)	168	250	261

* All material reduced 85% by extrusion then 75% by swaging; total reduction 96%. Heats 16 through 25 processed entirely at 1422°K (2100°F). Refer to the thermo-mechanical processing study for the fabrication details on heats 26 and 27.

** Prepared for the TMP study.

4. 1. 3 Optical Microstructure

Samples of heats 16 through 25 were annealed for 1 hour at temperatures ranging from 1589 to 1839°K (2400 to 2850°F). Changes of microstructure caused by heat treatment are shown in Figures 2 through 10. Certain general observations can be made. These are:

1. All alloys are recrystallized by annealing at 1589°K (2400°F).
2. An increasing annealing temperature causes the gradual elimination of fine precipitates. This is accompanied by development of coarse second phase particles located primarily at grain boundaries in the Cr-.50Ta(C,B) and carbide strengthened alloys, and large globular particles in the boride strengthened compositions.

Changes of microstructure and carbide stability caused by heat treatment were examined extensively for the Cr-.50TaC composition on previous work^(5,6). The elimination of fine precipitates and formation of a coarse grain boundary phase, which occurs at high annealing temperatures, corresponds to a change of carbide stability for the monocarbide to $Cr_{23}C_6$. Similar microstructure changes noted on this program for alloys containing 0.75 and 1.00 m/o TaC are an indication that an identical transition in carbide stability occurs in these compositions. It is likely that temperature influences carbide stability in a similar manner in the Cr-.75CbC composition. An analogous argument, based on previously obtained microstructure and phase stability data,^(6,8) can be presented for the boride strengthened alloys relating the change of particle morphology to a high temperature transition from stability of tantalum and columbium-rich phases* to Cr_4B . A relationship between microstructure and phase stability cannot be postulated from any reported data for the Cr-.50Ta(C,B) composition. However, an extraction of second phase material obtained from a specimen creep tested for 244 hours at 1422°K (2100°F) was identified by x-ray diffraction as consisting of Ta_2CrB_2 and TaC, not a complex tantalum carboboride. The development of coarse grain boundary and intragranular particles noted in this alloy

* Ta_2CrB_2 and Cb_2CrB_2 are the approximate formulas of actual strengthening borides formed in the Cr-TaB and Cr-CbB alloys.

after annealing at high temperatures (see Figure 2) might represent a transition to stability of Cr_{23}C_6 and Cr_4B or some complex $\text{Cr}_4(\text{C}, \text{B})$ phase.

Microstructural observations specific to certain alloys are:

1. Presence of large grey globular particles in the Cr-.50TaC alloy (Figure 3).
2. Evidence that heat treatment at 1839°K (2850°F) caused liquation in the Cr-.75CbC and Cr-.75CbB compositions (Figures 6 and 10).
3. A decrease in annealed grain size with increased TaB level (Figures 7-9).

Oxygen contamination was greatest in the Cr-.50TaC alloy, and the grey particles in its microstructure are probably globules of tantalum oxide. In situ examination by electron microprobe analysis did reveal high levels of tantalum and oxygen in these particles.

The conclusion that heat treatment at 1839°K (2850°F) caused liquation in the 0.75 m/o CbC and CbB compositions is based upon the eutectic-like appearance of the grain boundary constituent. By comparison, the alloys containing an identical level of TaC or TaB did not display any evidence of liquation after similar heat treatment.

Careful examination of Figures 7 through 9 reveals that the content of second phase generally increases with increasing TaB level. More effective boundary pinning may be the reason grain size and TaB level appear inversely related.

Hardness is plotted against annealing temperature in Figure 11 for each of the study compositions. The major decrease in this property after heat treatment at 1589°K (2400°F) results from recrystallization. The transition from stability of the tantalum and columbium phases to the Cr_{23}C_6 and Cr_4B compounds is believed responsible for the general increase of hardness with increasing annealing temperature above $\sim 1755^\circ\text{K}$ (2700°F). The tantalum and columbium contents of the

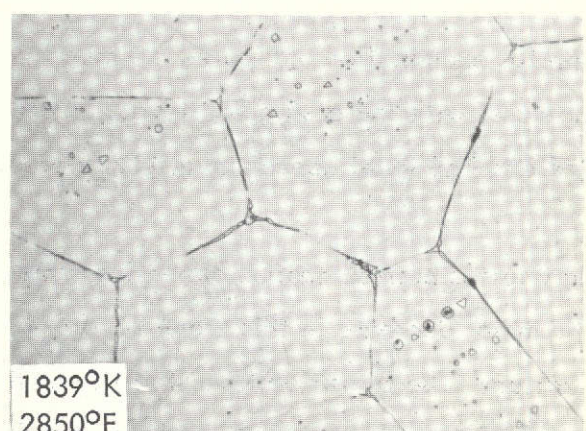
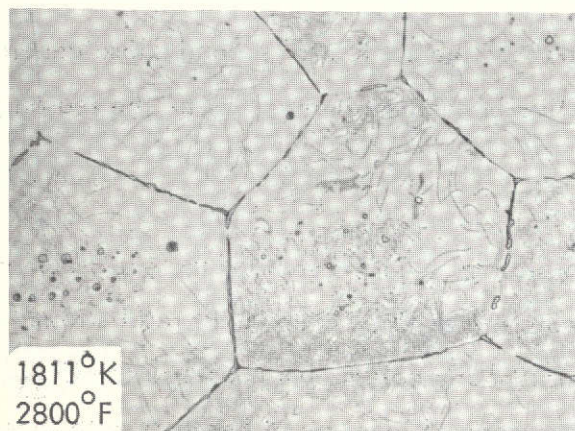
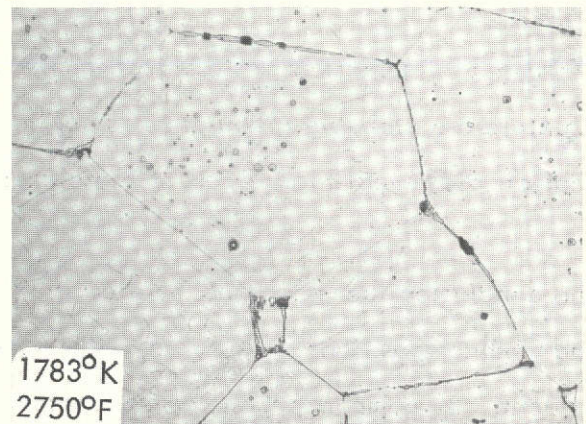
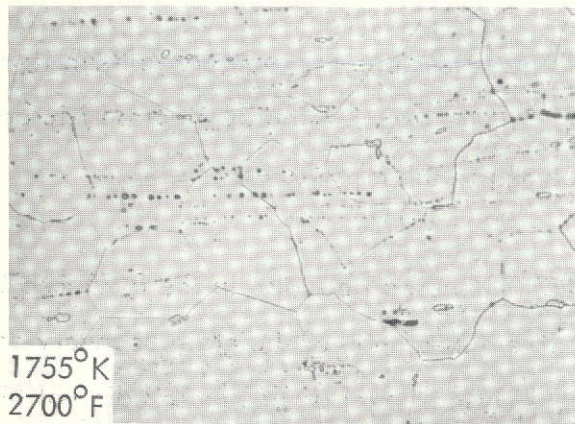
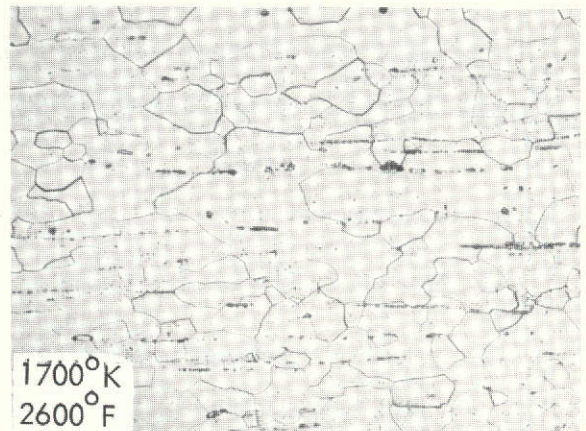
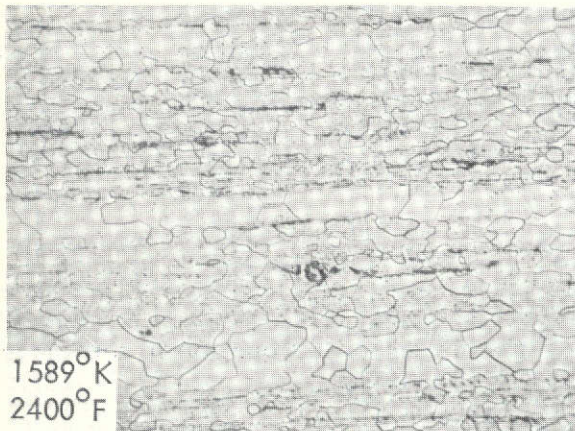


Figure 2. The Influence Heat Treatment for 1 Hour at 1589 to 1839°K (2400 to 2850°F) has on the Microstructure of the Cr-.5Ta(C,B) Alloy 250X

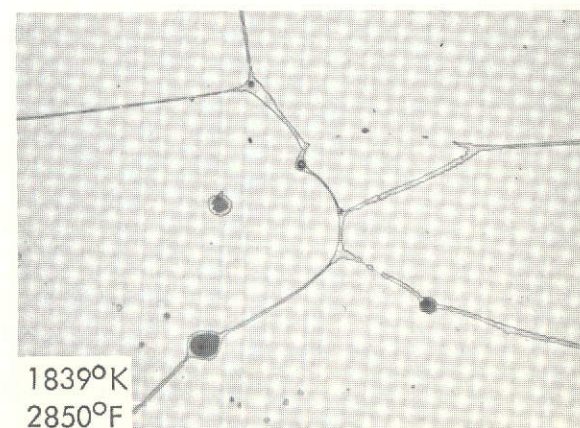
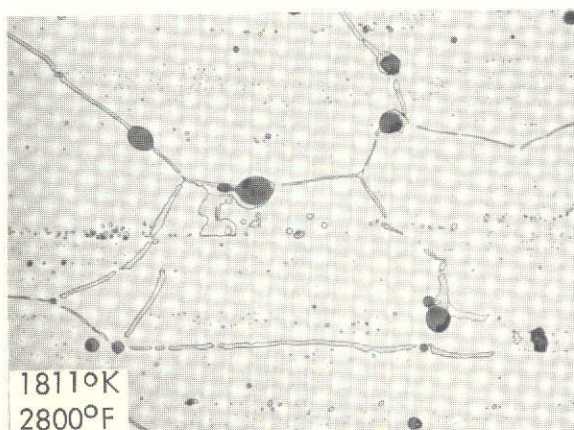
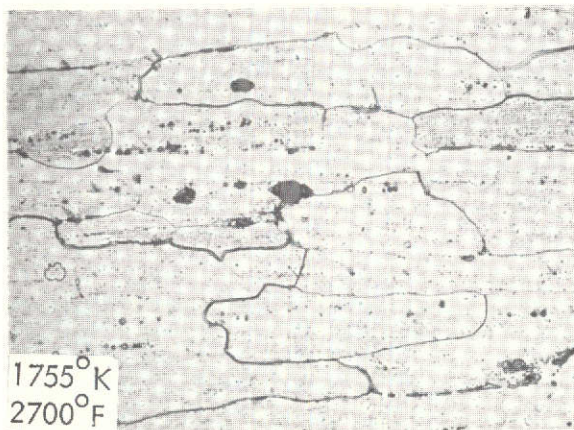
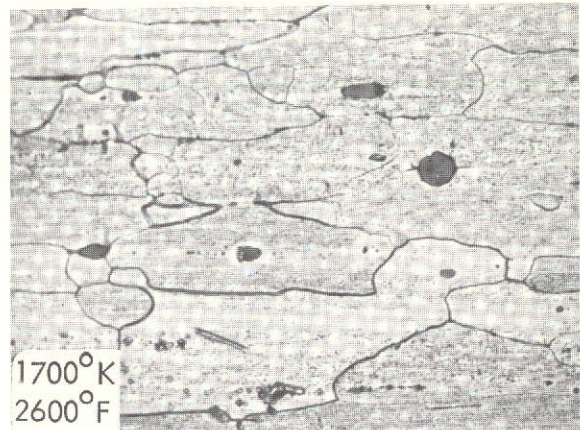
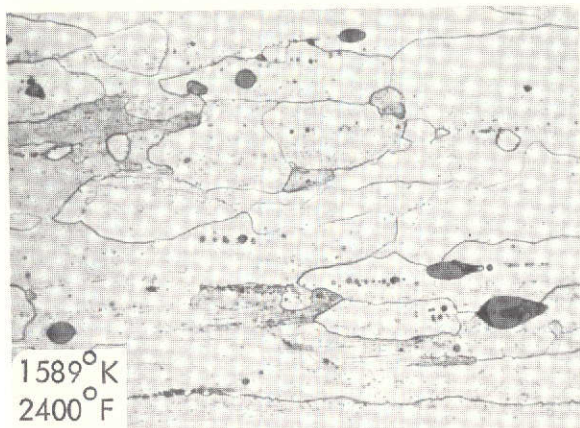


Figure 3. The Influence Heat Treatment for 1 Hour at 1589 to 1839°K (2400 to 2850°F) has on the Microstructure of the Cr-.5TaC Alloy - 250X
 Grey particles are probably oxides of tantalum resulting from severe oxygen contamination.

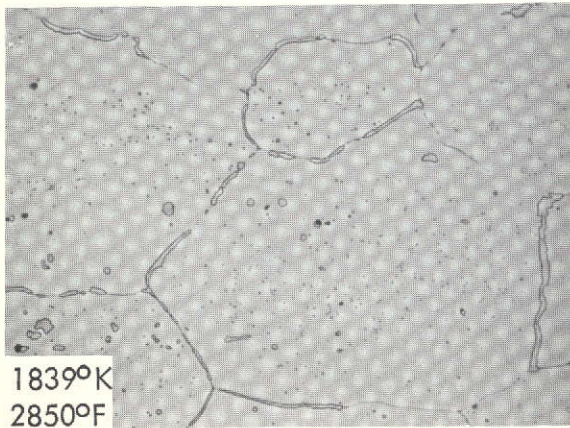
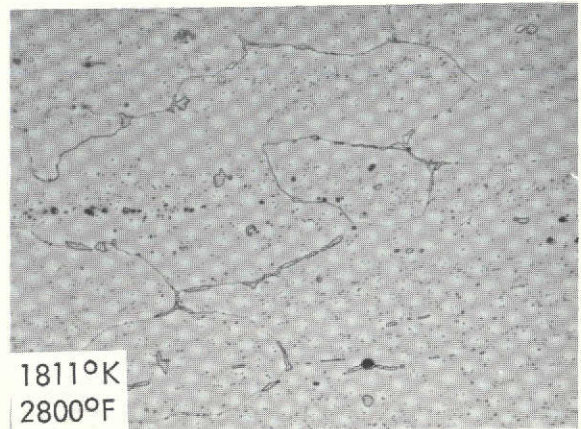
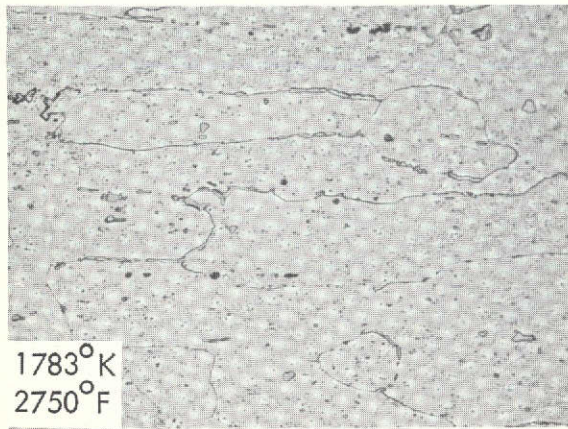
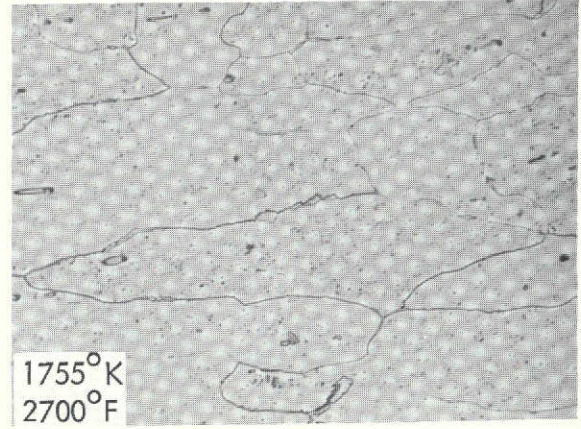
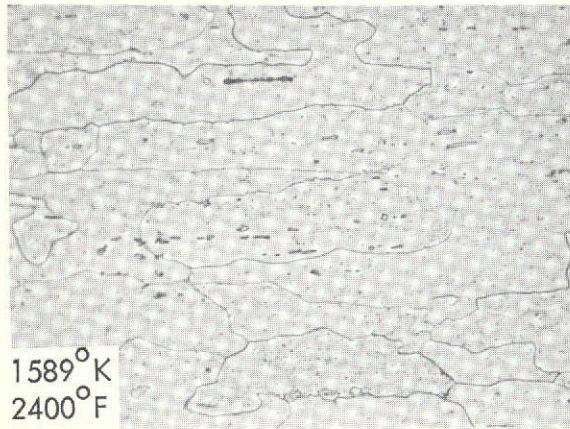


Figure 4. The Influence Heat Treatment for 1 Hour at 1589 to 1839°K (2400 to 2850°F) has on the Microstructure of the Cr-.75 TaC Alloy - 250X

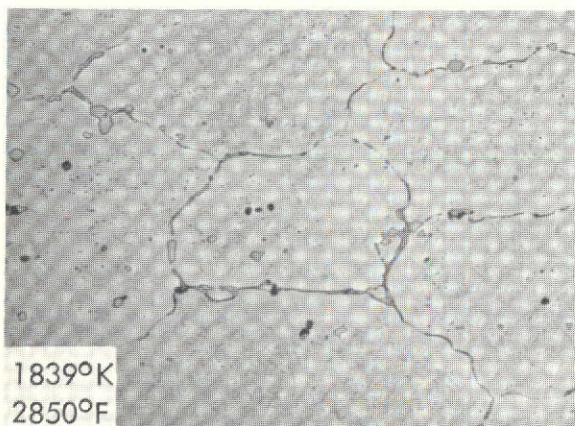
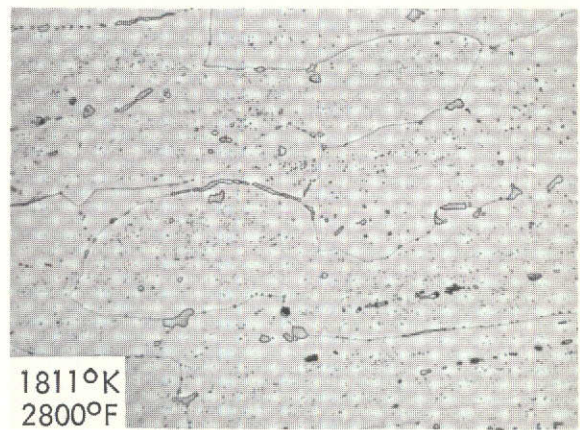
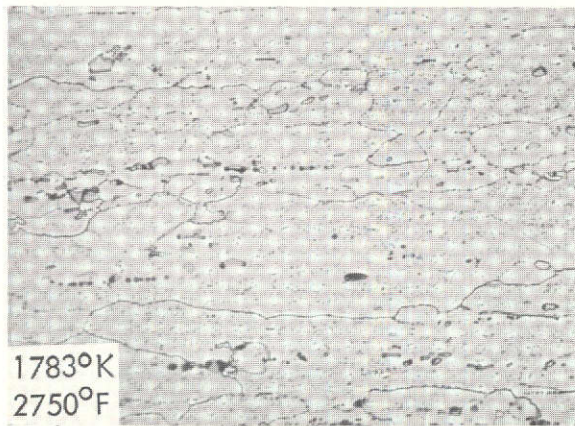
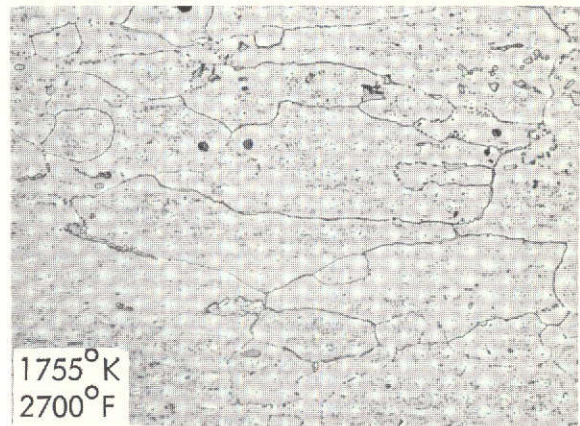
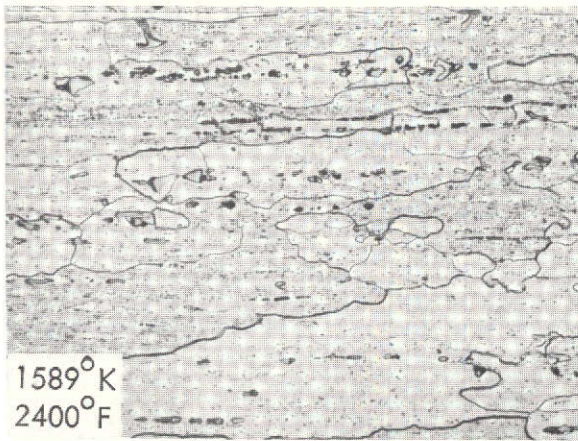


Figure 5. The Influence Heat Treatment for 1 Hour at 1589 to 1839°K (2400 to 2850°F) has on the Microstructure of the Cr-1.00 TaC Alloy - 250X

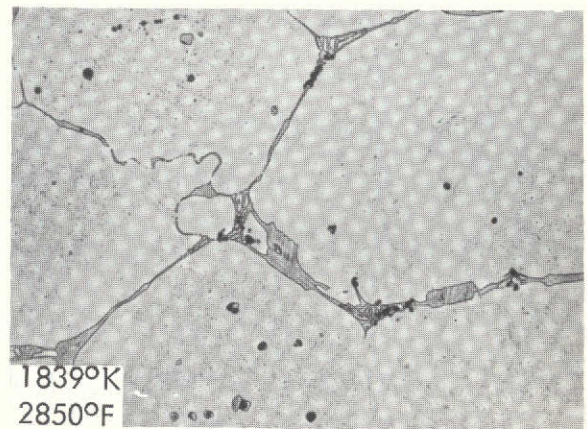
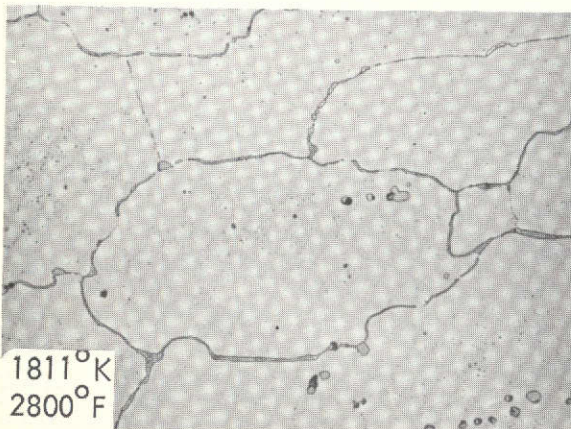
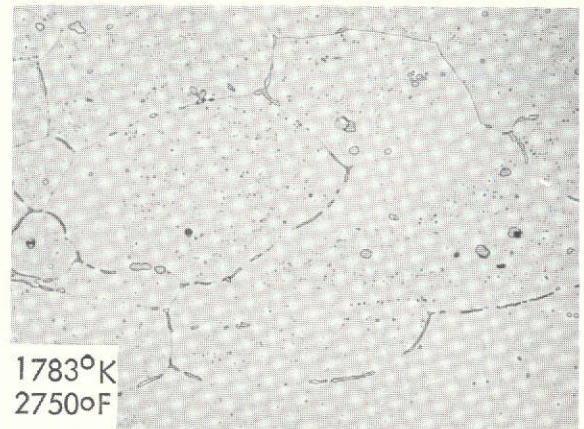
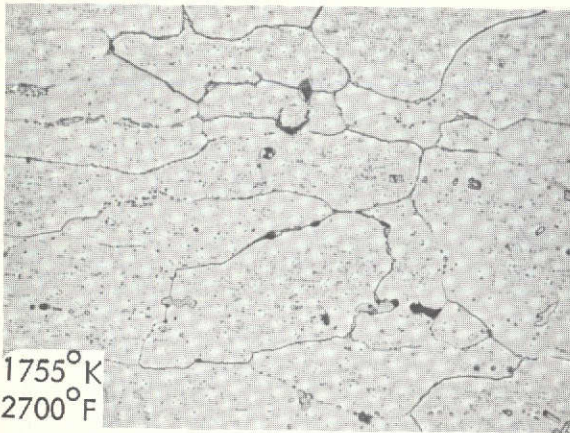
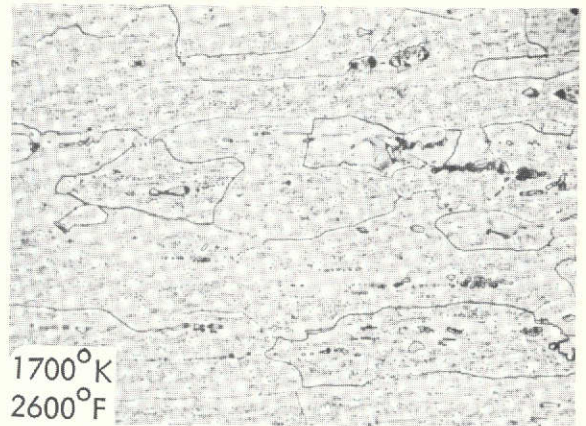
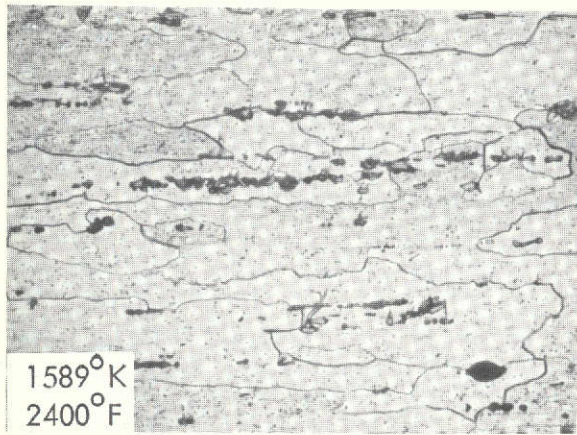


Figure 6. The Influence Heat Treatment for 1 Hour at 1589 to 1839°K (2400 to 2850°F) has on the Microstructure of the Cr-.75 CbC Alloy - 250X
Liquation at 1839°K is indicated by the eutectic-like grain boundary constituent.

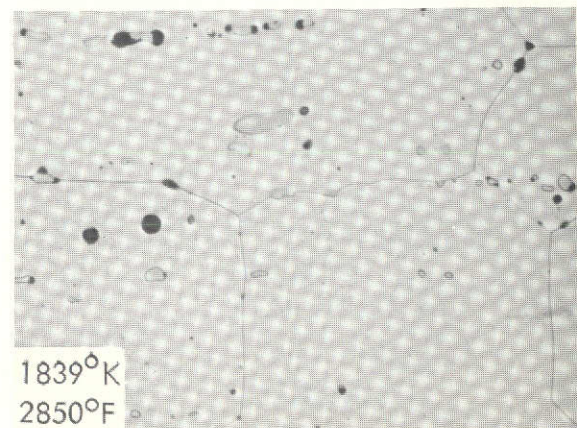
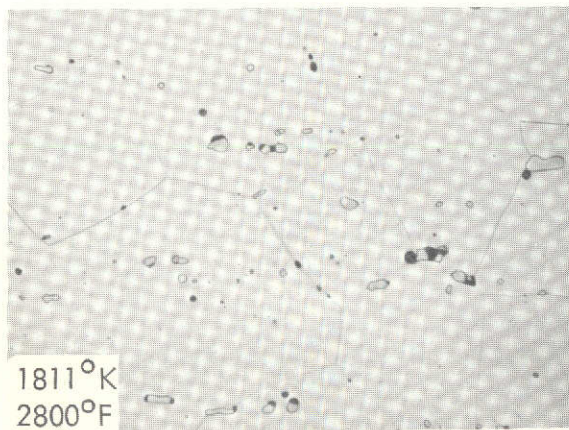
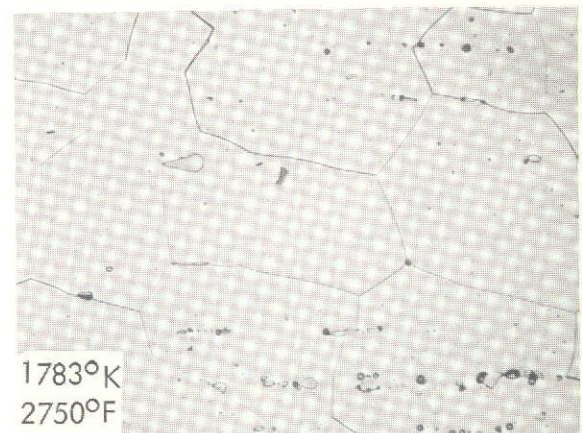
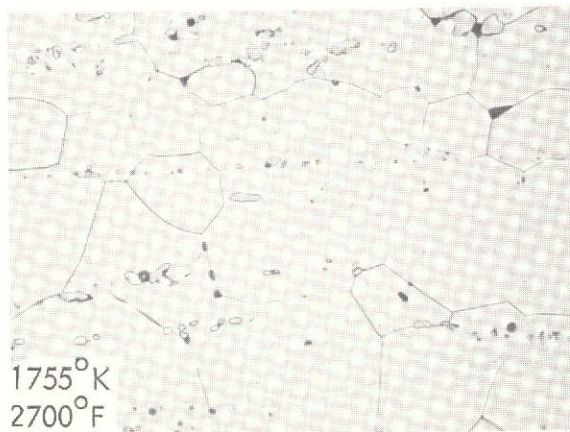
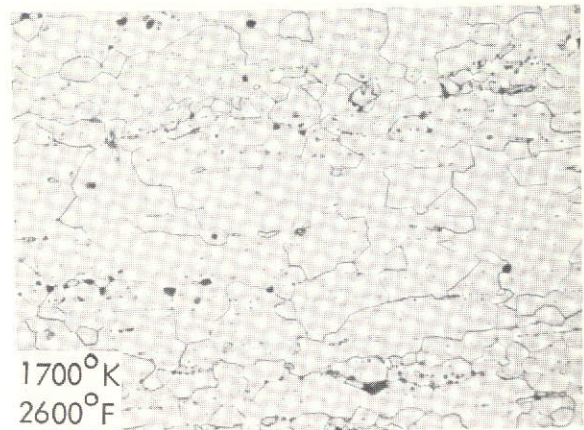
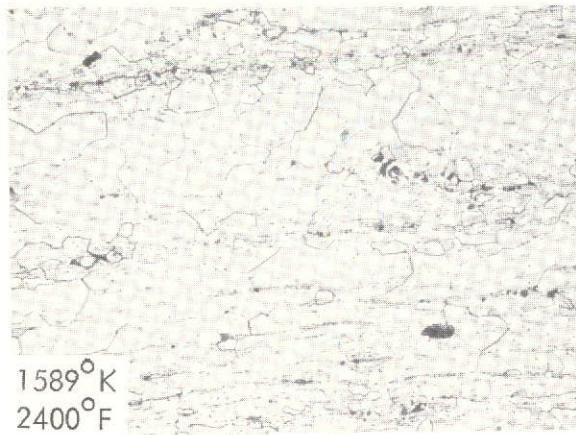


Figure 7. The Influence Heat Treatment for 1 Hour at 1589 to 1839°K (2400 to 2850°F) has on the Microstructure of the Cr-.5TaB Alloy - 250X

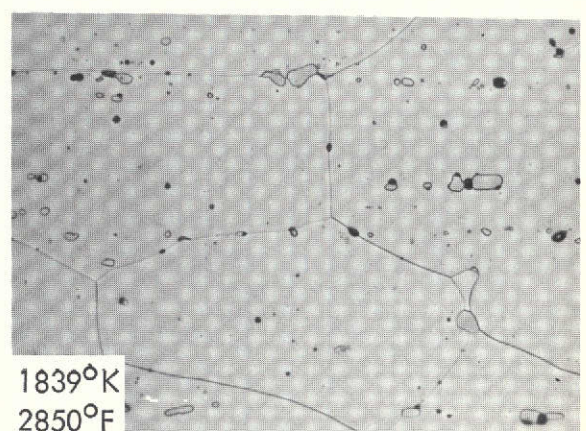
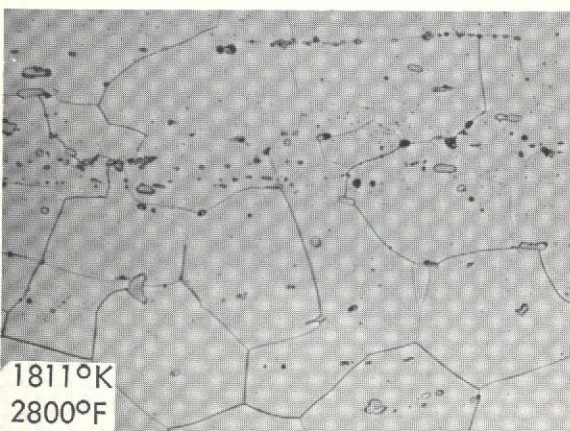
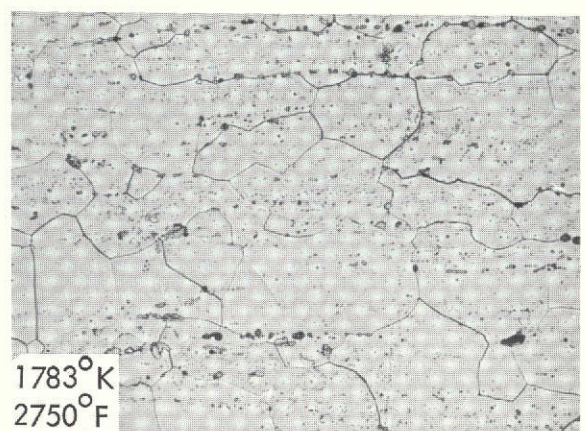
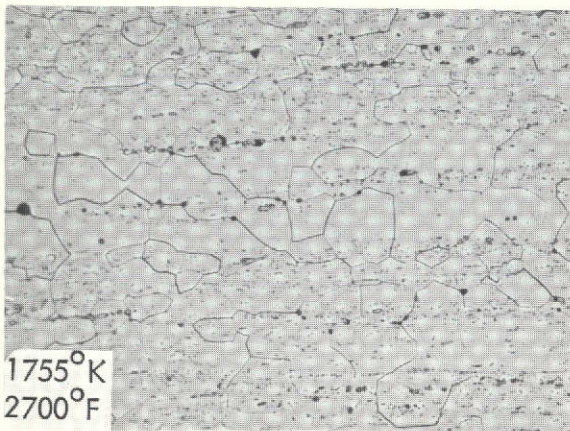
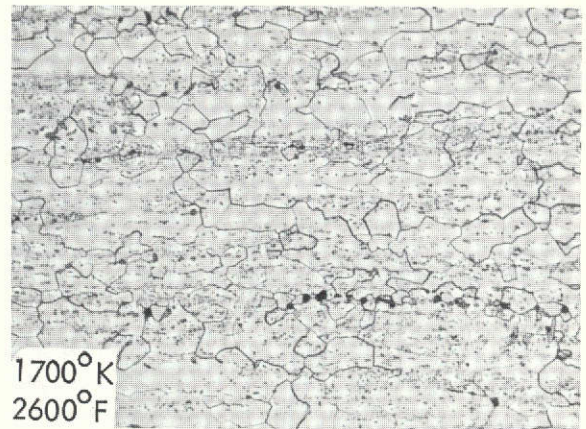
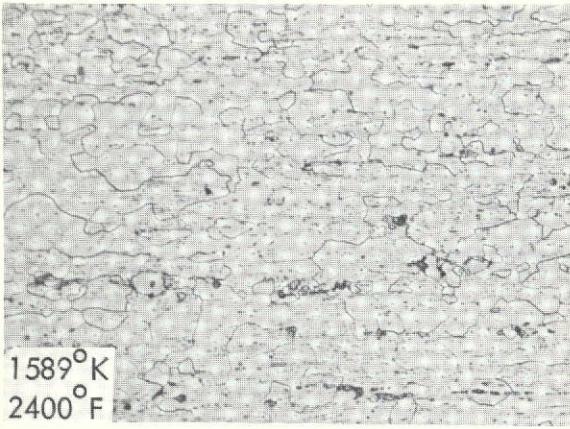


Figure 8. The Influence Heat Treatment for 1 Hour at 1589 to 1839°K (2400 to 2850°F) has on the Microstructure of the Cr-.75 TaB Alloy - 250X

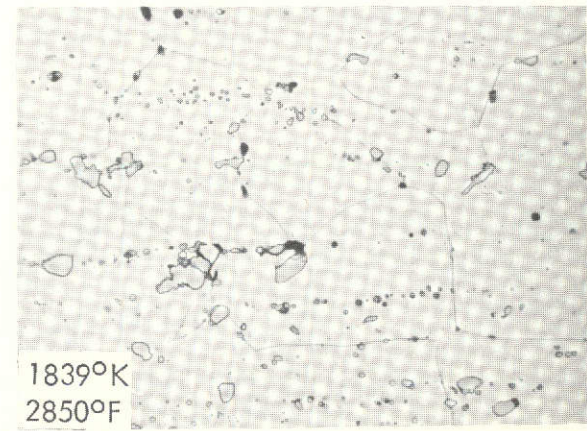
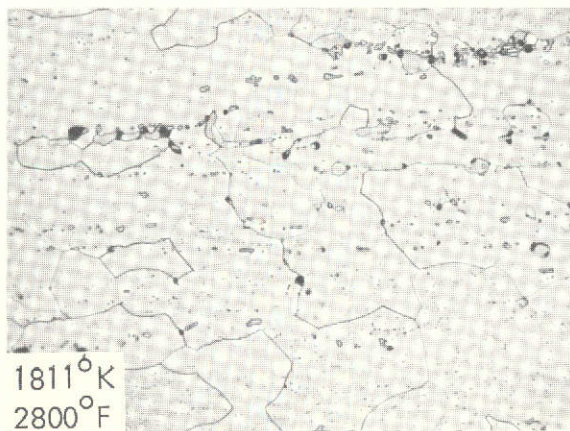
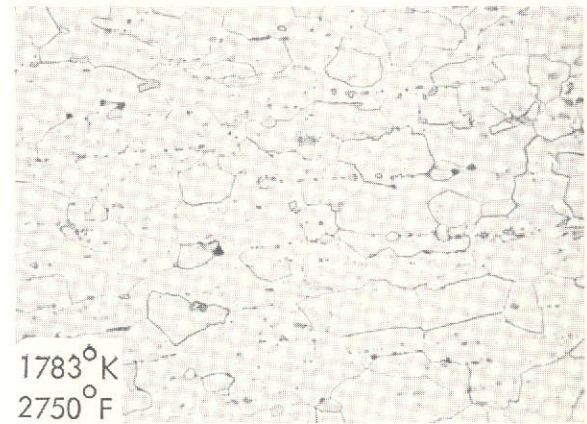
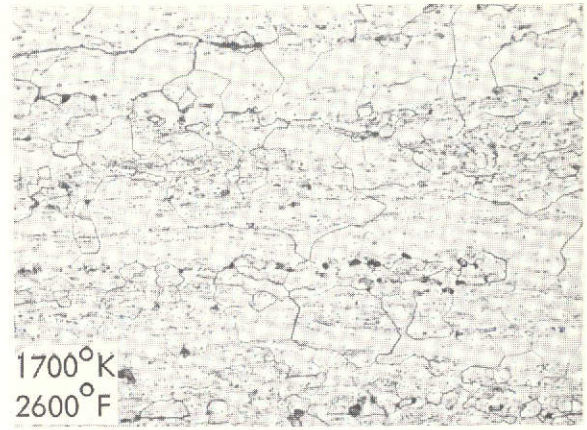
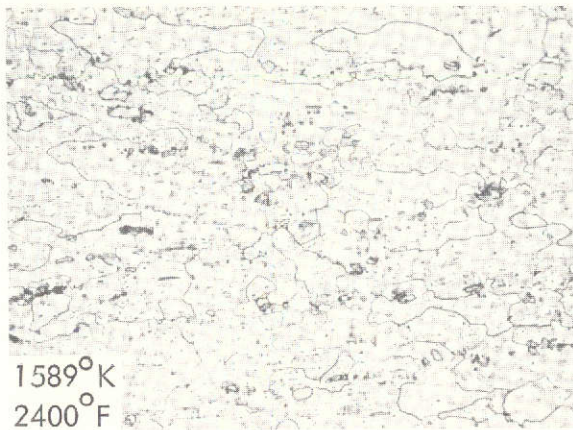


Figure 9. The Influence Heat Treatment for 1 Hour at 1589 to 1839°K (2400 to 2850°F) has on the Microstructure of the Cr-1.00 TaB Alloy - 250X

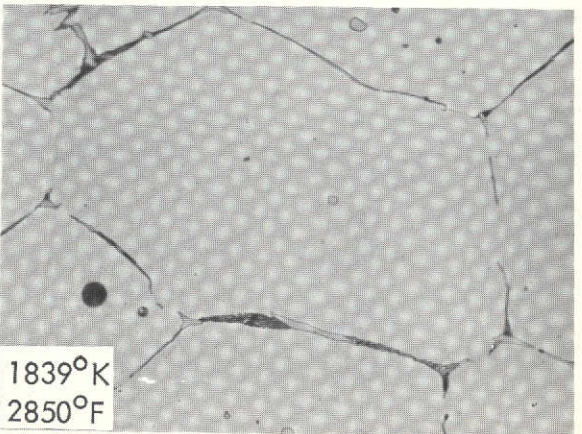
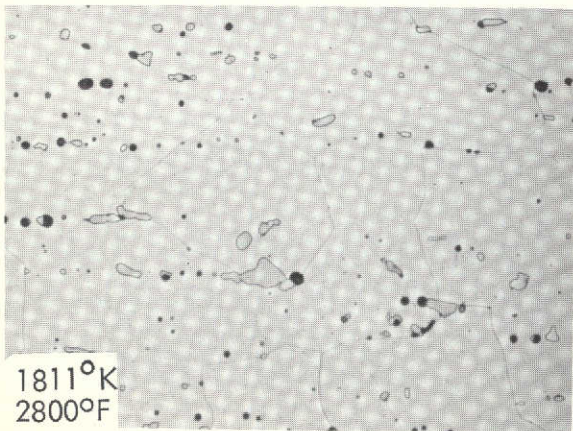
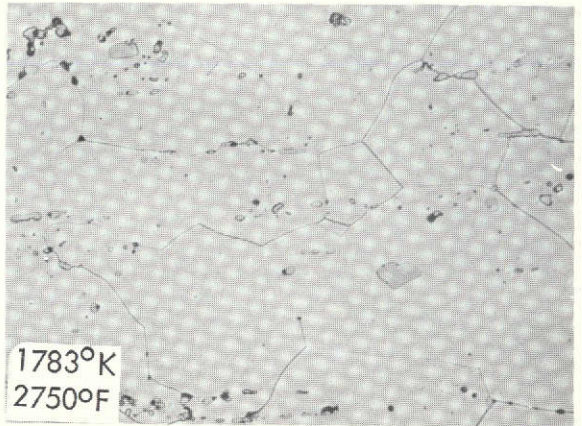
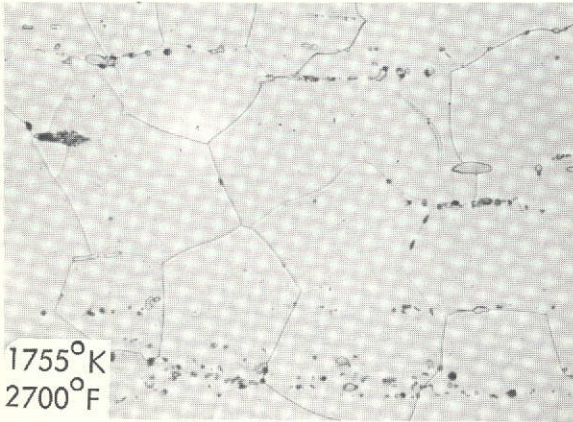
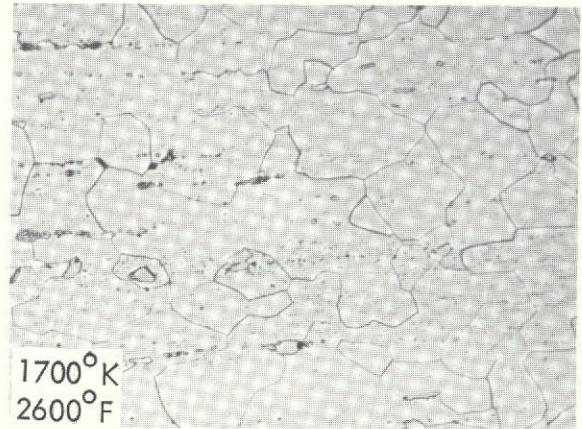
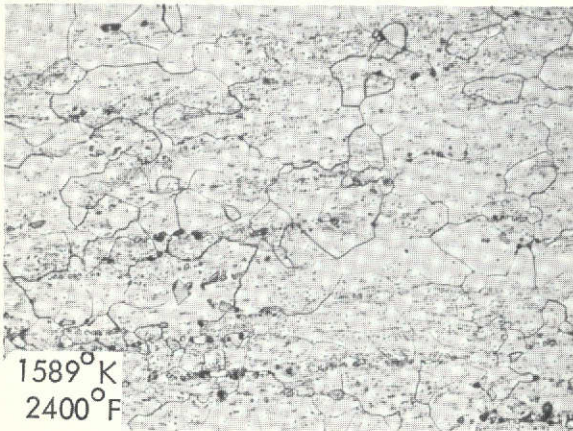


Figure 10. The Influence Heat Treatment for 1 Hour at 1589 to 1839°K (2400 to 2850°F) has on the Microstructure of the Cr-.75 CbB Alloy - 250X
Liquation at 1839°K is indicated by the eutectic-like grain boundary constituent.

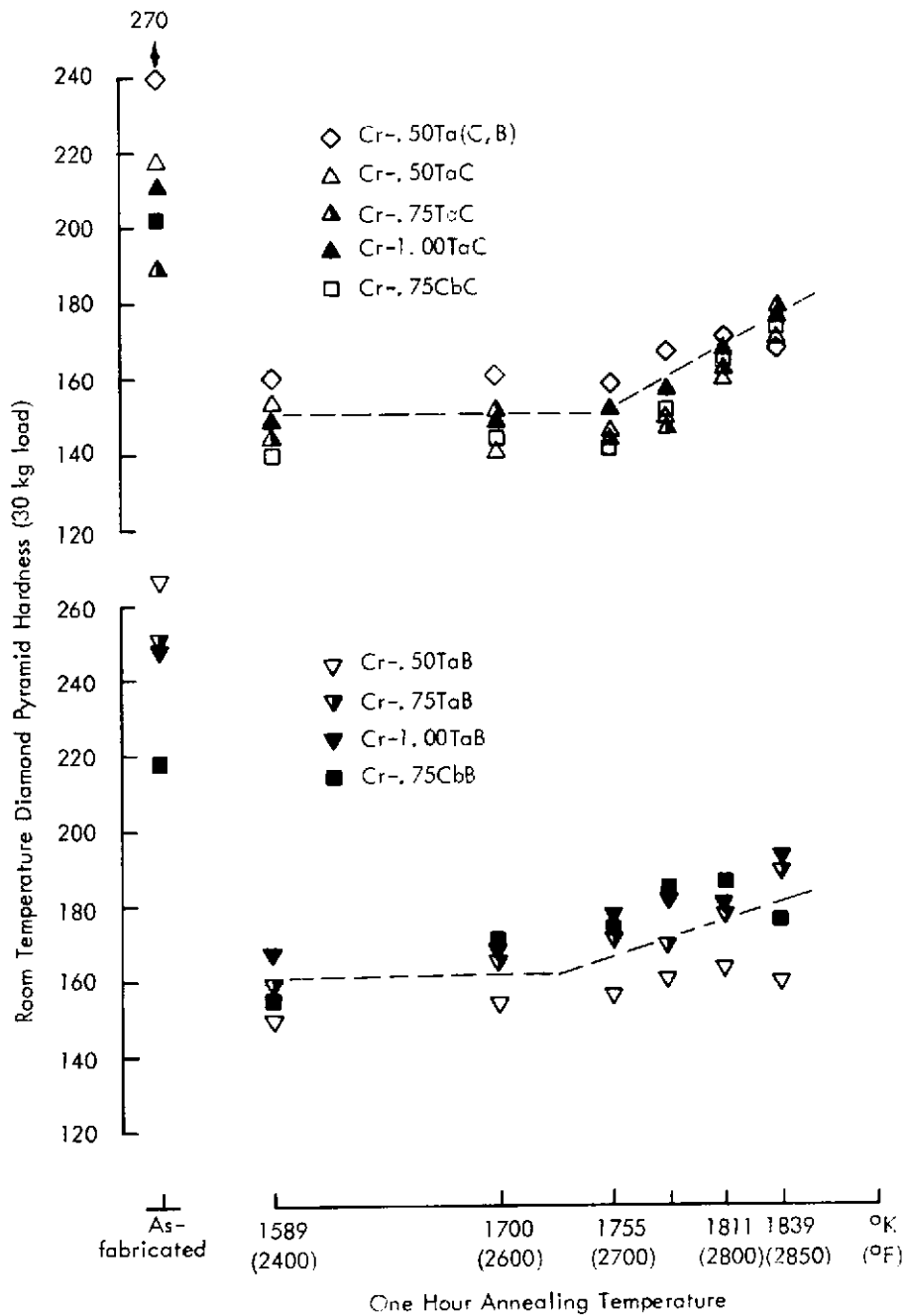
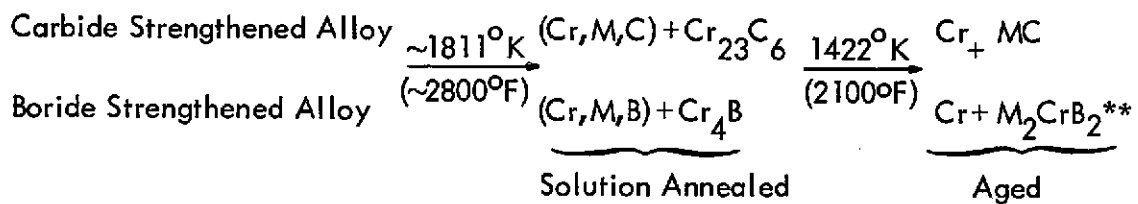


Figure 11. The Influence of Heat Treatment on Hardness of the Carbide and Boride Strengthened Alloys

alloys are solutioned by this change of phase stability resulting in an increase of hardness. A portion of the carbon and boron contents is undoubtedly also solutioned, contributing to the hardness increase.

4. 1. 4 Tensile Properties at 1422°K (2100°F)

Tensile properties were measured on the nine similarly fabricated alloys at 1422°K (2100°F). Data are reported in Table 3. Every composition was tested as-fabricated and in a solution annealed and aged condition. Six alloys were tested after recrystallization for one hour at 1589°K (2400°F). Solution annealing and aging treatments which optimize creep strength, a property to be discussed in a latter section, were used. These treatments as applied to the chromium alloys cause microstructural changes which are analogous but not identical to those commonly typified by the heat treatment of commercial aluminum alloys. The solution annealing treatments, for example, do not produce a single phase solid solution condition. Instead, the microstructure of material so heat treated consists of Cr₂₃C₆ or Cr₄B particles in a matrix of chromium containing the alloying metal and some carbon or boron in solid solution*. Aging actually solutiones the Cr₂₃C₆ or Cr₄B compounds while precipitation of the tantalum and columbium strengthening phases occurs simultaneously. This second heat treatment has previously been referred to as carbide or boride interchange aging^(5,6). The phase changes involved are summarized below for typical alloys.



* Refer to the preceding section on optical microscopy.

** M₂CrB₂, M = Ta or Cb, is the approximate formula for actual borides formed in the Cr-TaB and Cr-CbB alloys.

Table 3. Tensile Properties of the Carbide and Boride Strengthened Alloys Determined at 1422°K (2100°F)

Composition m/o	Material Condition	0.2% Yield		U. T. S.		El (%)	Area Red (%)
		MN/m ²	(ksi)	MN/m ²	(ksi)		
Cr-.50Ta(C, B)	A *	434	62.9	486	70.4	18.3	61.4
	B	154	22.2	172	25.2	40.7	87.4
	C	213	30.8	248	35.9	23.8	75.0
Cr-.50TaC	A	216	31.3	234	33.9	20.4	53.8
	C	191	27.6	209	30.3	9.6	19.3
Cr-.75TaC	A	176	25.5	188	27.2	20.9	78.5
	B	84	12.2	124	18.0	44.6	88.6
	C	209	30.4	226	32.7	19.5	79.7
Cr-1.00TaC	A	194	28.2	212	30.7	22.6	72.2
	B	95	13.7	128	18.6	46.8	85.8
	C	180	26.1	195	29.3	20.9	72.2
Cr-.75CbC	A	169	24.5	178	25.8	22.0	72.7
	C	149	21.6	172	24.8	22.7	70.7
Cr-.50TaB	A	345	50.0	373	54.0	20.1	62.5
	B	127	18.4	161	23.3	56.3	89.5
	C	130	18.9	193	27.9	46.5	78.0
Cr-.75TaB	A	331	48.0	350	50.7	20.1	65.7
	B	149	20.0	176	25.4	47.6	83.2
	C	159	23.1	213	30.9	41.4	79.1
Cr-1.00TaB	A	324	46.9	337	48.9	21.6	61.0
	B	152	21.9	192	27.6	46.9	80.0
	C	137	19.8	210	30.5	38.6	74.5
Cr-.75CbB	A	264	38.3	275	39.9	33.4	75.9
	C	173	25.1	241	34.9	38.6	73.5

* A - As-fabricated

B - Annealed 1 hr/1589°K (2400°F)

C - Annealed 0.25 hr/1839°K (2850°F) + 3 hr/1422°K (2100°F) for Cr-TaC alloys
0.25 hr/1811°K (2800°F) + 3 hr/1422°K (2100°F) for other compositions

The highest 1422°K (2100°F) tensile strength was obtained on the Cr-.50Ta(C,B) alloy in the as-fabricated condition, 486 MN/m² (70.4 ksi). Tensile strengths of the TaB strengthened alloys in this condition ranged from 337 to 373 MN/m² (48.9 to 54.0 ksi), and for compositions containing TaC from 188 to 234 MN/m² (27.2 to 33.9 ksi). Differences in strength obtained as a function of TaC and TaB levels are probably too small to positively state that definite effects were measured. However, it can be concluded that increasing the amount of these phases from 0.5 to 1.0 m/o certainly does not bring about any major tensile strength improvement. The Cr-.75CbB alloy displayed a 275 MN/m² (39.9 ksi) tensile strength as-fabricated, while only 178 MN/m² (25.8 ksi) was measured on the Cr-.75CbC composition.

The 1422°K (2100°F) tensile strengths of as-fabricated materials were related more to carbide or boride chemistry than to amount present. An arrangement of alloying phases in decreasing order of their strengthening potential is: Ta(C,B), TaB, CbB, TaC, and CbC. Improvement in high temperature strength by replacing carbon with boron in dispersion hardened chromium-base alloys has been previously reported^(5,6). However, it is apparent that an even greater level of strength can be attained by alloying with both carbon and boron.

Differences in tensile strengths measured after a solution anneal and age treatment were not as pronounced as noted for as-fabricated material and ranged from a low of 172 MN/m² (24.8 ksi) for the Cr-.75 CbC composition to a high of 248 MN/m² (35.9 ksi) for the Cr-.50Ta(C,B) alloy. Whereas in the as-fabricated condition strengths of the Cr-TaB alloys were far superior to those containing TaC, in the solution annealed and aged condition these alloys displayed a similar level of tensile strength; ~200 MN/m² (~30 ksi).

Three arbitrarily chosen compositions, Cr-.75TaC, Cr-1.00TaC, and Cr-.5TaB were tested in a simple recrystallized condition achieved by annealing for one hour at 1589°K (2400°F). These tests provide a minimum base line to which strength in other conditions can be compared. Carbide and boride dispersion strengthened chromium-base alloys have previously been shown

to display poor tensile and creep strengths as-recrystallized^(5,6), so emphasis was not placed on evaluation in this condition.

The Cr-.50TaC alloy displayed a pronounced loss of tensile ductility in the solution treated and aged condition. The ductility of this alloy was comparable to the others when tested as-fabricated, ~20% elongation but decreased to ~10% after solution treatment and aging. This property was unaffected or increased by heat treatment on all alloys. Contamination by oxygen was most serious in the Cr-.50TaC composition (Table 1), and the loss of ductility after heat treatment is believed related to this. An identical heat treatment induced ductility loss was observed on previous work in Cr-CbC compositions similarly contaminated with oxygen^(5,6).

4.1.5 Creep Properties at 1422°K (2100°F)

Creep data were gathered on the nine experimental alloys at 1422°K (2100°F) and are reported in Table 4. Each alloy was tested as-fabricated and in one or two solution annealed and aged conditions at a stress of 104 MN/m² (15 ksi). Selected high strength alloys were also tested in the solution annealed and aged condition at higher stress levels. Major observations on creep behavior are:

1. The as-fabricated alloys did not display significant differences in creep properties. Creep rates were relatively high and ranged from 0.3 to 7%/hr. causing failure in ~1 day for the strongest alloy and ~1 hour for the weakest.
2. In the majority of cases solution annealing and aging treatments brought about a one or two order of magnitude improvement in creep rates and rupture times.
3. Based on limited data, it appears that substituting Cb for Ta in carbide or boride strengthened alloys does not yield any improvement in creep strength.

Table 4. Creep Behavior of the Carbide and Boride Strengthened Alloys Determined at 1422°K (2100°F)

Nominal Composition m/o	Mat'l. Cond. *	Test Stress		Minimum Creep Rate (%/hr)	Rupture Life (hrs.)	Rupture Ductility		3rd Stage Transition	
		MN/m ²	(ksi)			(% EI)	(% RA)	(hrs.)	(% EI)
Cr-.50Ta(C,B)	A	104	15.0	0.286	15.1	36.0	75.5	4.3	2.0
	C	104	15.0	0.002	>278.5**	--	--	--	--
	C	124	18.0	0.003	325.9	17.0	72.5	209	1.5
	C	138	20.0	0.002	423.2	10.0	57.7	276	1.1
	C	145	22.0	0.003	244.4	15.0	62.1	130	1.2
	C	173	25.0	0.006	194.5	12.0	57.9	126	1.6
Cr-.50TaC	A	104	15.0	0.505	11.1	18.0	37.6	3.5	2.5
	C	104	15.0	0.060	21.3	8.0	18.2	--	--
	C'	104	15.0	0.009	50.0	2.0	7.6	32	1.5
	C'	104	15.0	--	32.3	3.0	4.6	--	--
Cr-.75TaC	A	104	15.0	4.2	2.5	29.0	83.2	1.5	7.9
	C	104	15.0	0.94	6.5	29.0	86.6	2.0	2.4
	C'	104	15.0	0.002	393.7	9.0	57.6	--	--
	C'	114	16.5	0.003	295.0	11.0	71.9	--	--
	C'	124	18.0	0.025	38.9	17.0	89.4	17.0	1.4
	C'	124	18.0	0.003	151.5	10.0	65.9	120	1.3
	C'	138	20.0	0.008	104.0	12.0	58.5	85	1.7
	C'	159	23.0	0.025	24.0	16.0	83.9	20	1.3
Cr-1.00TaC	A	104	15.0	4.2	3.5	35.0	75.2	1.7	8.8
	C	104	15.0	0.024	56.6	21.0	84.8	26.0	2.0
	C'	104	15.0	0.003	277.2	15.0	84.6	162	1.3
	C'	114	16.5	0.017	77.9	18.0	88.9	--	--
	C'	124	18.0	0.065	28.6	19.0	87.2	--	--
	C'	131	19.0	0.124	12.7	19.0	82.9	5.0	1.0
	C'	138	20.0	0.299	7.9	20.0	83.9	2.4	1.5
Cr-.75CbC	A	104	15.0	7.0	1.2	30.0	80.2	.6	5.0
	C	104	15.0	0.009	119.2	16.0	81.4	103	2.2
	C'	104	15.0	0.022	56.3	16.0	75.3	48	1.8

Table 4 (Continued)

Nominal Composition m/o	Mat'l. Cond. *	Test Stress		Minimum Creep Rate (%/hr.)	Rupture Life (hrs.)	Rupture Ductility		3rd Stage Transition	
		MN/m ²	(ksi)			(% El)	(% RA)	(hrs.)	(% El)
Cr-.50TaB	A	104	15.0	0.32	14.8	35.0	76.4	6	3.4
	C	104	15.0	0.004	186.4	18.0	74.4	120	1.3
	C'	104	15.0	0.006	125.0	17.0	68.9	70	1.1
	C	114	16.5	0.009	125.4	16.0	65.9	80	1.3
	C	124	18.0	0.018	86.1	13.0	67.0	58	2.2
	C	124	18.0	0.008	130.8	13.0	65.5	80	1.4
	C	138	20.0	0.019	83.1	15.0	66.9	54	3.4
	C	165	22.5	0.027	56.9	17.0	63.5	31	3.5
Cr-.75TaB	A	104	15.0	0.283	31.2	35.0	69.2	11	4.2
	C	104	15.0	0.030	79.4	28.0	78.7	--	--
Cr-1.00TaB	A	104	15.0	--	18.2	40.0	67.4	--	--
	C	104	15.0	0.170	46.0	38.0	79.3	--	--
	C'	104	15.0	--	62.1	26.0	79.9	--	--
Cr-.75CbB	A	104	15.0	1.0	11.7	44.0	78.0	--	--
	C	104	15.0	0.032	82.7	29.0	77.4	25	1.5

* A - As-fabricated

C - Annealed 0.25 hr/1811°K (2800°F) + 3 hr/1422°K (2100°F)

C' - Annealed 0.25 hr/1839°K (2850°F) + 3 hr/1422°K (2100°F)

** Test stopped at 278.5 hrs.

4. A small increase of solutioning temperature from 1811 to 1839°K (2800 to 2850°F) made a major improvement in creep properties of the Cr-.75TaC and Cr-1.00TaC alloys but had either an insignificant or deliterious influence on the creep behavior of other compositions.

5. The Cr-.50Ta(C,B) composition displayed the most outstanding creep strength.

The first three observations on creep behavior have been reported for similar carbide and boride strengthened chromium-base alloys evaluated on other work^(5,6).

The strong dependency of creep properties on solutioning temperature displayed by the Cr-.75TaC and Cr-1.00TaC alloys implies that a major increase in TaC solubility occurs between the temperatures of 1811 and 1839°K (2800 and 2850°F). Microstructural conditions developed in these alloys by heat treatment are shown in Figures 4 and 5 and appear to confirm this conclusion. Substantially fewer intragranular TaC particles are present in the alloys after annealing at 1839°K (2850°F) as opposed to 1811°K (2800°F) or lower.

Heat treatment failed to significantly improve the creep properties of the Cr-.50TaC alloy over that observed for as-fabricated material regardless of solutioning temperature. This is a somewhat surprising result in light of the pronounced influence thermal treatment had on the creep strength of the Cr-.75TaC and Cr-1.00TaC compositions. The very high level of oxygen contamination in the Cr-.50TaC alloy is believed responsible for its failure to respond to heat treatment; see Table 1. This conclusion is based on an identical observation made on similarly severely oxygen contaminated Cr-CbC alloys^(5,6). It is believed that a portion of the alloying metal in proportion to the level of oxygen contamination is tied up as an oxide and prevented from entering the precipitate strengthening reactions. A loss of elevated temperature ductility, noted previously in the discussion of tensile properties of the Cr-.50TaC alloy and attributed to oxygen contamination, was also observed on creep tested material.

Mechanical properties have been reported for a heat of Cr-.50TaC containing 1/3 the level of oxygen contamination of material prepared on this program^(5,6). A sample solution treated at 1839°K (2850°F) then aged at 1422°K (2100°F) displayed a 186 hour rupture life when tested at 104 MN/m² and 1422°K (15 ksi and 2100°F). This level of creep resistance compares to a rupture life of 394 hours for Cr-.75TaC and 277 hours for Cr-1.00TaC measured on this program; see Table 4. It follows that a plot of creep resistance against precipitate level for the 0.5 to 1.0 m/o TaC range would show a maximum in the vicinity of ~0.75 m/o. By comparison, data presented in Table 4 for Cr-TaB alloys reveals that creep strength is greatest at 0.5 m/o TaB and decreases as the level of this precipitate is increased to 1 m/o. The magnitude of creep strengthening achieved through use of the individual TaC and TaB compounds, however, is far below that obtained by combining these phases in the Cr-.50Ta(C,B) composition.

Creep rate and rupture life data obtained on the four most creep resistant experimental compositions are plotted against test stress in Figures 12 and 13. Data are presented for solution annealed and aged specimens of the Cr-.50Ta(C,B), Cr-.50TaB, Cr-.75TaC, and Cr-1.00TaC alloys. Lines fitted to the creep rate data favor the higher values which are considered to be more accurately determined; see Figure 12. Average fit lines are drawn through the rupture life information; Figure 13. One of the six points plotted for the Cr-.75TaC alloy has been ignored since it falls well outside of the most consistent data trend. The two highest test stress points shown for the Cr-.50Ta(C,B) alloy were obtained on material produced for the thermomechanical processing study. These data are reported in Table 8.

The empirical expression relating the creep rate of pure metals to stress level and material characteristics⁽⁹⁾, given below, forms the basis for presenting the stress dependency of this property on log-log coordinates.

$$\text{Creep Rate} = \dot{\epsilon} = S \left(\frac{\sigma}{E} \right)^n D$$

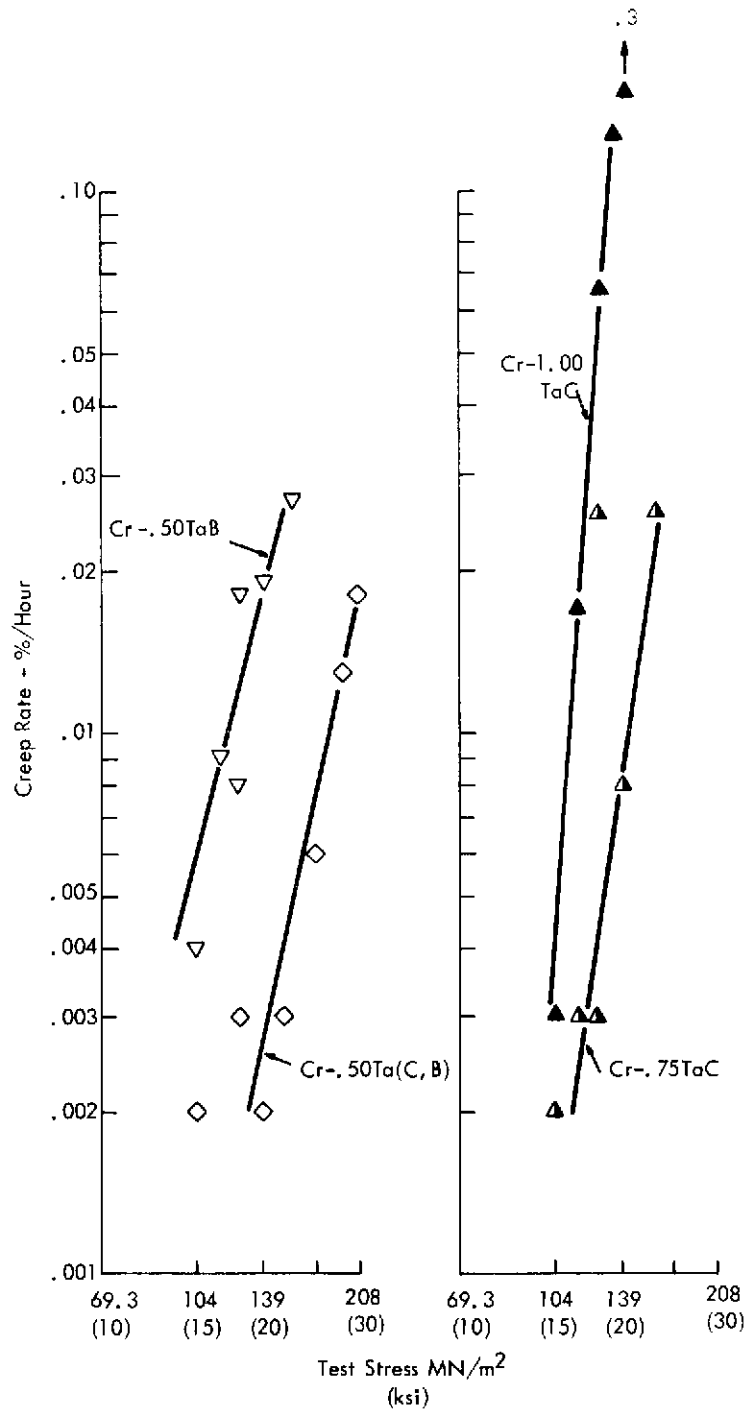


Figure 12. The Influence of Test Stress on the Creep Rates Observed at 1422°K (2100°F) for the Four Most Creep Resistant Experimental Compositions. (Data obtained on solution annealed and aged material; see Table 4).

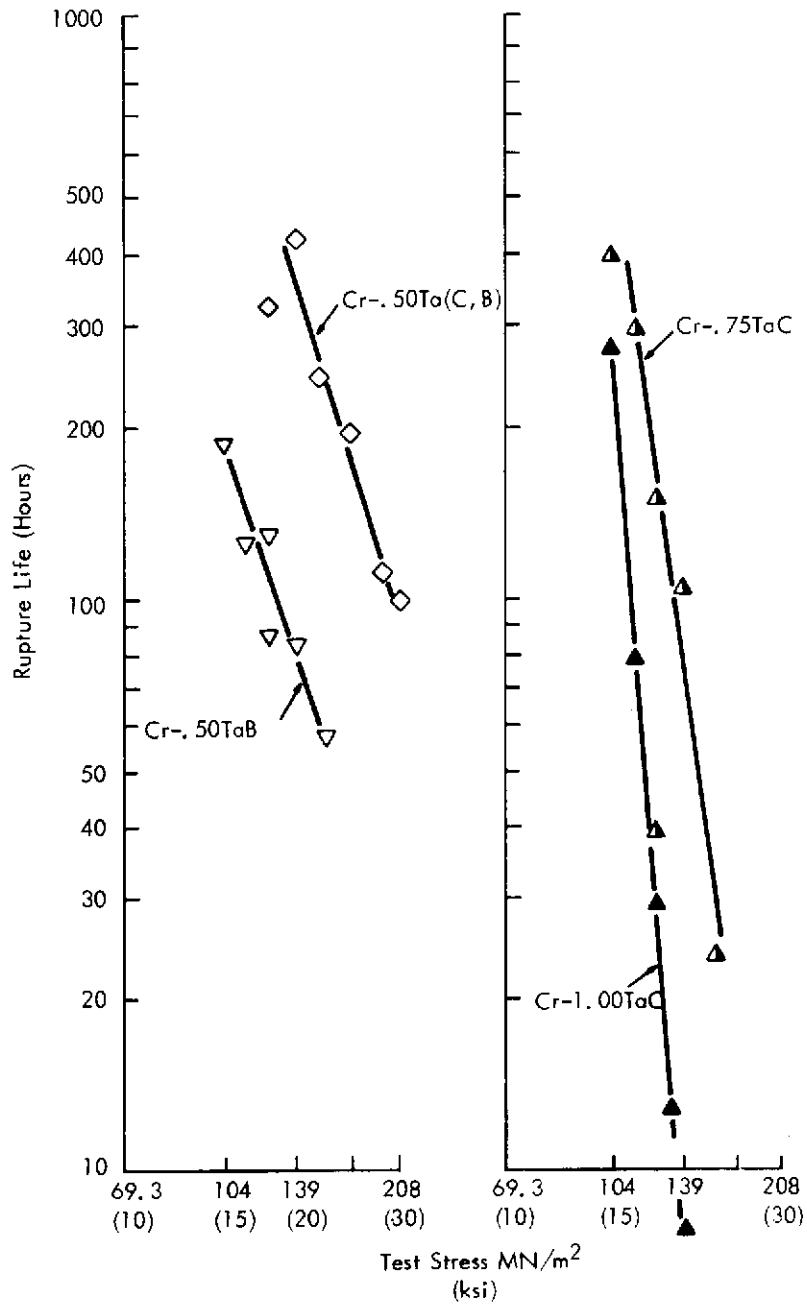


Figure 13. The Influence of Test Stress on the Rupture Times Observed at 1422°K (2100°F) for the Four Most Creep Resistant Experimental Compositions. (Data obtained on solution annealed and aged material; see Table 4)

In this relationship, structure considerations, i. e., grain size, dislocation array, etc., make up the S term, σ refers to the test stress, n is a numerical exponent, and E and D are the test materials' elastic modulus and self diffusivity. For a set of constant temperature data obtained on a material tested in one metallurgical condition, this expression reduces to:

$$\Delta \log \dot{\epsilon} = n \Delta \log \sigma$$

The following expression is obtained if creep rate and rupture life are assumed to be inversely related:

$$\Delta \log (\text{rupture life}) = -n \Delta \log \sigma$$

Consequently, the absolute magnitude of n is directly related to the influence stress level has on creep resistance.

Values of the stress dependency exponent, n, determined for the four most creep resistant compositions are listed in Table 5. They were calculated from the slopes of the data plotted in Figures 12 and 13. Similar and lowest n values were obtained for the Cr-.50Ta(C,B) and Cr-.50TaB alloys. A stress dependency exponent of 3 to 5 might be a reasonable estimate for these compositions. The Cr-.75TaC and Cr-1.00TaC alloys displayed n values of approximately 7 and 13, respectively. The different effects of stress on creep resistance cannot be rationalized on any mechanistic basis without additional information. However, the observed behavior might be associated in some way with the amount of precipitate present in the alloys since the n values do increase progressively as this level changes from 0.5 to 1.0 m/o.

A Larson-Miller plot of rupture data is presented in Figure 14 for the four most creep resistant chromium-base compositions. Included in the Figure is a band indicating the rupture stress level of the currently strongest superalloys. It represents materials such as MAR-M200, TRW-NASA VIA, NASA WAZ 20, and TD-Nickel tested in their optimum conditions. The

Table 5. A Comparison of the Stress Dependency Parameters Displayed by the Four Highest Creep Strength Alloys*

Composition m/o	Stress Dependency Factors**	
	$n(\sigma, \dot{\epsilon})$	$n(\sigma, R. L.)$
Cr-.50Ta(C, B)	4.6	3.2
Cr-.50TaB	3.9	2.9
Cr-.75TaC	7.0	6.9
Cr-1.00TaC	13.2	12.4

* Materials tested in the solution annealed and aged condition.

$$** \quad n(\sigma, \dot{\epsilon}) = \frac{\Delta \log \dot{\epsilon}}{\Delta \log \sigma} \quad (\text{Figure 12})$$

$$n(\sigma, R. L.) = \left| \frac{\Delta \log (\text{Rupture Life})}{\Delta \log \sigma} \right| \quad (\text{Figure 13})$$

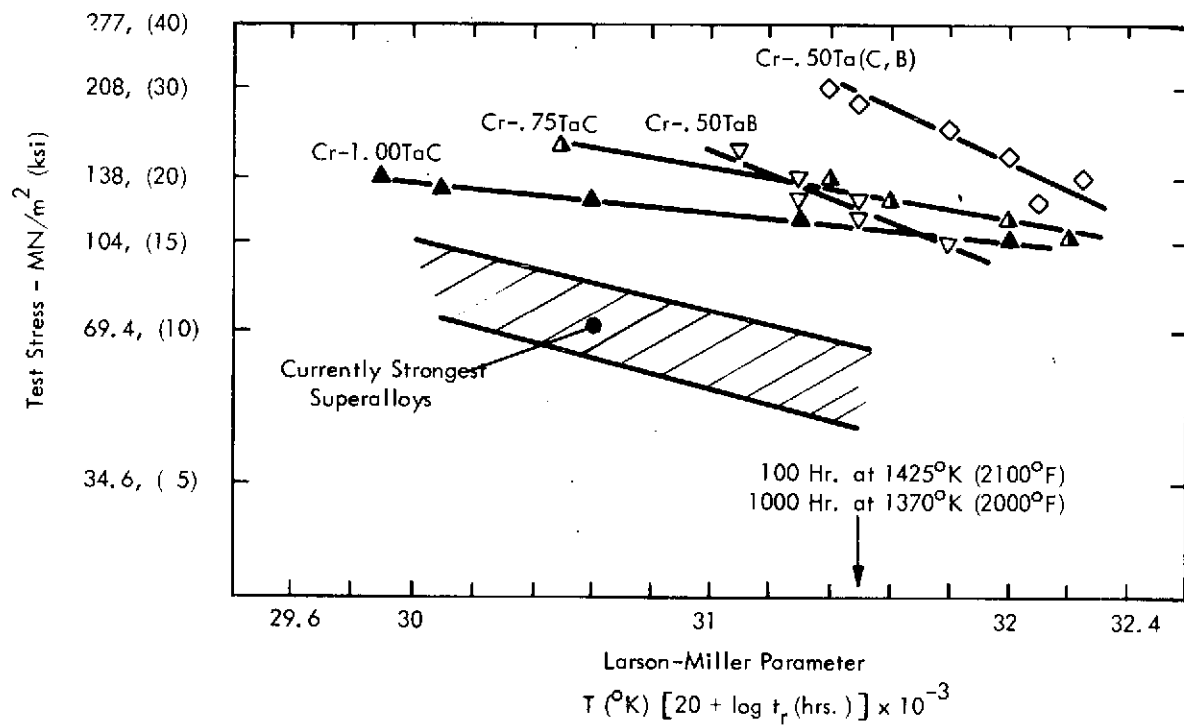


Figure 14. A Larson-Miller Comparison of Rupture Strengths of the Most Superior Superalloys and Experimental Chromium-base Compositions. (Chromium-base alloys tested in the solution annealed and aged condition.)

chromium-base materials developed on this program display rupture strengths for superior to the best available superalloy. For example, the 1000 hour rupture strengths of the chromium-base alloys range from 104 to 208 MN/m² at 1370°K (15 to 30 ksi at 2000°F). The strongest superalloy will display a similar rupture resistance at approximately 69.4 MN/m² (10 ksi).

4.1.6 Ductile-to-Brittle Transition Behavior

Estimates were made of the temperatures at which each experimental alloy underwent a change from ductile-to-brittle behavior. This was accomplished by determining the temperature dependence of tensile ductility from 0.05 cm/min (0.02 inch/minute) strain rate tests. Because creep strength would be a critical property if these alloys were to ever be considered for advanced turbine applications, their ductile-to-brittle characteristics were evaluated in the metallurgical condition which optimizes this property, i. e., the solution annealed and aged condition.

Ductile-brittle data are presented in Table 6. Values of ductile-to-brittle transition temperatures were estimated from the plots of reduction of area against temperature shown in Figure 15. No individual alloy displayed a markedly superior low temperature ductility, and DBTT estimates for the nine compositions spanned only 422 to 644°K (300 to 700°F), indicating composition had a minor influence on the property.

4.1.7 Precipitation of the Strengthening Phases

(Ta, Cr)₃B₂ and (Cb, Cr)₃B₂, Ta/Cr ~ Cb/Cr ~ 2, are the actual chemical formulas of the strengthening phases formed in the Cr-Ta-B and Cr-Cb-B alloys*. These are tetragonal compounds having similar lattice parameters; a ~ 5.9 x 10⁻¹⁰ m (5.9 Å), c ~ 3.2 x 10⁻¹⁰ m (3.2 Å). By comparison, face-centered cubic monocarbides of tantalum and columbium containing little if any chromium in solid solution form in Cr-Ta-C and Cr-Cb-C compositions. Lattice parameters of these monocarbides are also similar, a ~ 4.5 x 10⁻¹⁰ m (4.5 Å). Knowledge of the structure

* A discussion of the identification of these compounds is presented as a separate section under "Experimental Program and Discussion".

Table 6. Low Temperature Tensile Properties of the Carbide and Boride Strengthened Alloys

Heat Treated for Optimum Stress-Rupture Strength*

Composition m/o	Test Temp.		Elongation		Area Red. (%)	0.2% Yield		U. T. S.		DBTT***	
	(°K)	(°F)	%Uniform	%Total		MN/m ²	(ksi)	MN/m ²	(ksi)	(°K)	(°F)
Cr-.50Ta(C,B)	532	500	4.0	4.0	4.7	235	34.1	376	54.5**	532	500
	588	600	6.6	6.6	7.7	227	32.9	390	56.5**		
Cr-.50TaC	476	400	2.1	2.1	1.8	282	40.9	400	57.9**	532	500
	532	500	5.0	5.0	6.0	279	40.4	418	60.6**		
	644	700	6.9	9.7	21.3	285	41.3	424	61.3		
Cr-.75TaC	532	500	0.7	0.7	0.2	314	45.4	349	50.6**	644	700
	616	650	1.1	1.1	1.1	325	46.8	380	54.8		
	700	800	6.0	9.5	20.7	294	42.6	444	64.3		
Cr-1.00TaC	420	300	1.3	1.3	1.2	276	40.0	356	51.6**	476	400
	532	500	6.4	6.4	11.0	273	38.0	422	60.9		
	644	700	9.2	17.6	53.3	251	36.3	410	59.4		
Cr-.75CbC	532	500	2.4	2.4	0.9	263	38.0	365	52.9**	588	600
	588	600	3.8	3.8	3.7	287	41.6	407	59.0**		
	644	700	8.3	10.6	13.5	272	39.3	425	61.6		
Cr-.50TaB	420	300	3.2	3.2	3.6	197	28.5	343	49.6**	532	500
	532	500	5.3	5.3	5.2	172	24.8	336	48.7**		
	644	700	15.2	23.3	41.5	163	23.6	344	49.8		
Cr-.75TaB	420	300	5.3	5.3	2.9	223	32.3	391	56.7**	443	350
	532	500	10.2	10.2	12.9	211	30.5	410	59.4**		
	644	700	16.0	24.2	37.3	223	32.3	391	56.7		
Cr-1.00TaB	420	300	4.2	4.2	5.2	257	37.2	443	64.1**	420	300
	532	500	14.6	14.6	17.2	223	32.3	438	63.4**		
	644	700	12.9	20.7	61.0	195	29.3	410	59.3		
Cr-.75CbB	532	500	3.0	3.0	2.5	220	31.8	369	53.4**	644	650
	588	600	4.3	4.3	4.0	212	30.6	383	55.4**		
	644	700	8.3	8.3	9.0	199	28.8	398	57.7**		

* Annealed 0.25 hr/1839°K (2850°F) + 3 hr/1422°K (2100°F) for the Cr-TaC alloys
0.25 hr/1811°K (2800°F) + 3 hr/1422°K (2100°F) for the other compositions

** Specimen fractured before reaching an ultimate strength

*** Ductile-to-brittle transition temperature. The approximate temperature at which % reduction of area equals 5%. (Figure 15)

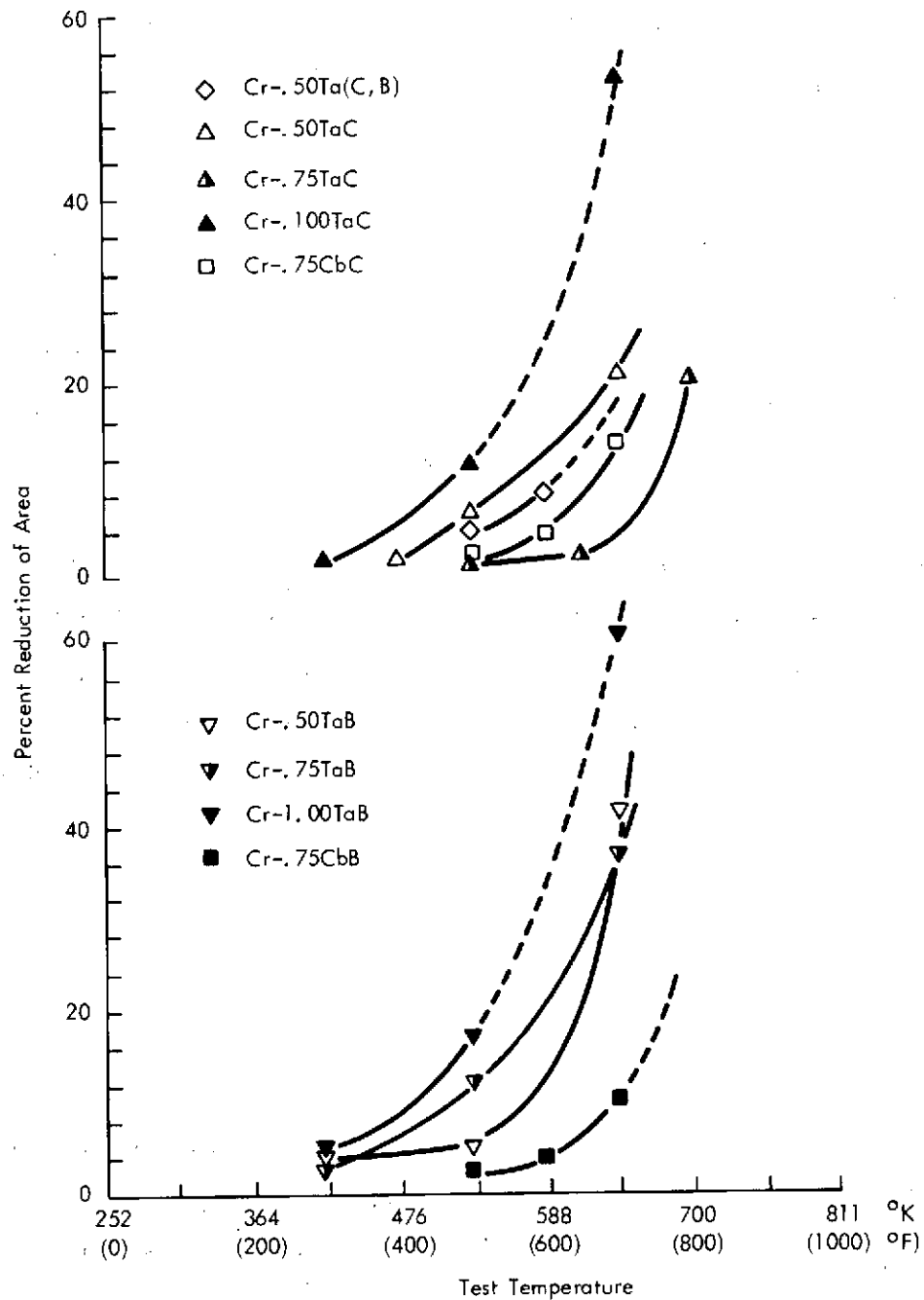


Figure 15. The Influence of Test Temperature on Tensile Reduction of Area Observed on the Carbide and Boride Strengthened Alloys. (Materials tested in the solution annealed and aged condition; see Table 6)

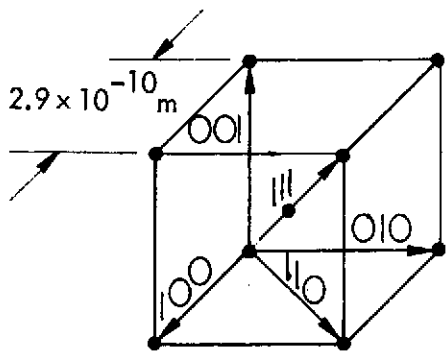
and parameters of these phases allows likely habit plane and direction relationships for coherency in a chromium matrix to be predicted. Some estimates of likely coherency relationships are made below based upon minimizing lattice mismatch on simple (low indice) matrix and precipitate planes.

Dimensions along several low indice crystallographic directions are noted in Figure 16 for chromium and the M_2CrB_2 and MC phases. Chromium atoms are shown at the corners and centers of (001) planes in the M_2CrB_2 unit cell which is consistent with the atomic arrangement reported by Beattie for this boride type⁽¹⁰⁾. The face-centered cubic arrangement of tantalum or columbium atoms is shown for the MC phase.

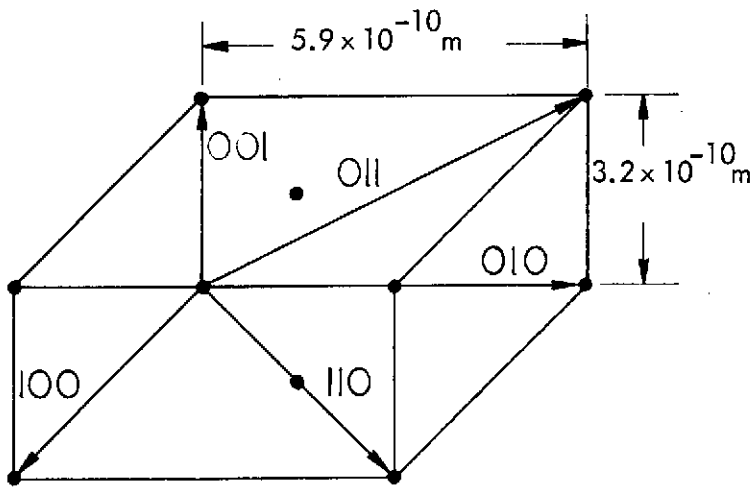
Comparing the structure of chromium with that of the M_2CrB_2 compound reveals nearly identical [001] dimensions. Furthermore, the [100] and [010] dimensions in the M_2CrB_2 structure are each approximately twice the corresponding dimensions in chromium, and the [110] in this metal is essentially equivalent to the chromium atom spacing along this direction in the boride. As a consequence, the following Cr- M_2CrB_2 coherency relationship is suggested.

$$\begin{array}{ccc} \underline{\text{Cr}} & & \underline{M_2CrB_2} \\ (001) & // & (001) \\ [110] & // & [110] \end{array}$$

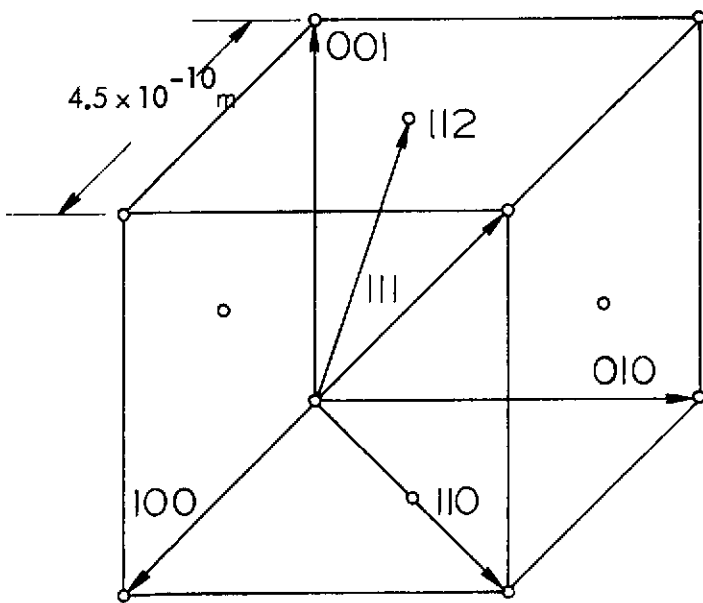
A comparison of chromium and the MC structure reveals a similarity between the [100] dimension in the metal and the spacing of metal atoms along the direction [110] in the carbide. The [110] dimension in the chromium lattice is also similar to that of [100] in the carbide. If the chromium and carbide lattices are superimposed to align these crystallographic directions, the habit relationship given below is obtained.



$[hkl]$	Length $\times 10^{10}m$	Chromium
100,010,001	2.9	(BCC)
110	4.1	
111	5.0	



$[hkl]$	Length $\times 10^{10}m$	M_2CrB_2
100,010	5.9	(Tetra)
001	3.2	
110	8.3	
011	7.1	



$[hkl]$	Length $\times 10^{10}m$	MC
100,010,001	4.5	(FCC)
110	6.4	
111	7.8	
112	5.5	

Figure 16. The Unit Cells and Lattice Dimensions of Chromium, and the M_2CrB_2 and MC Phases ($M = Ta$ or Cb)

<u>Cr</u>		<u>MC</u>
(001)	//	(001)
[100]	//	[110]

Precipitation of TaC in chromium according to the above relationship was established by electron microscopy through analysis of matrix and precipitate diffraction data. The Cr-0.50TaC alloy, solution treated then aged for 3 hours at 1422°K (2100°F) - the condition used to evaluate high temperature strength, was examined. The microstructure observed in a foil of (110) orientation is presented in Figure 17. This condition is characterized by formation of these TaC platelets. Those on edge and aligned along [110] lie parallel to (001) matrix planes. Particles having a rectangular appearance lie parallel to {100} planes which are at 45° to the foil plane.

4.1.8 Oxidation Behavior at 1422°K (2100°F)

The air oxidation characteristics of compositions selected to cover a wide range of yttrium and precipitate contents were examined at 1422°K (2100°F). Data were gathered on tests of 70 to 100 hours duration. In all cases weight gain displayed a parabolic relationship with test time after a few hours of exposure. Data obtained, reduced to parabolic rate constants, are presented in Table 7.

Values obtained for oxidation rate constants ranged from 0.2 to 2 mgs/cm²-hr^{1/2}. Although yttrium contents spanning from 0.01 to 0.17 a/o were represented by the alloys chosen, no simple relationship between oxidation rate and level of this element was observed. The data, however, do appear to reveal a relationship to the amount and type of strengthening precipitate present. Alloys containing tantalum carbide displayed a change of oxidation rate from ~1 to ~2 mgs/cm²-hr^{1/2} as the level of this phase increased from 0.5 to 1.0 m/o. By comparison, a similar change in TaB level resulted in little significant change in oxidation rate. Furthermore,

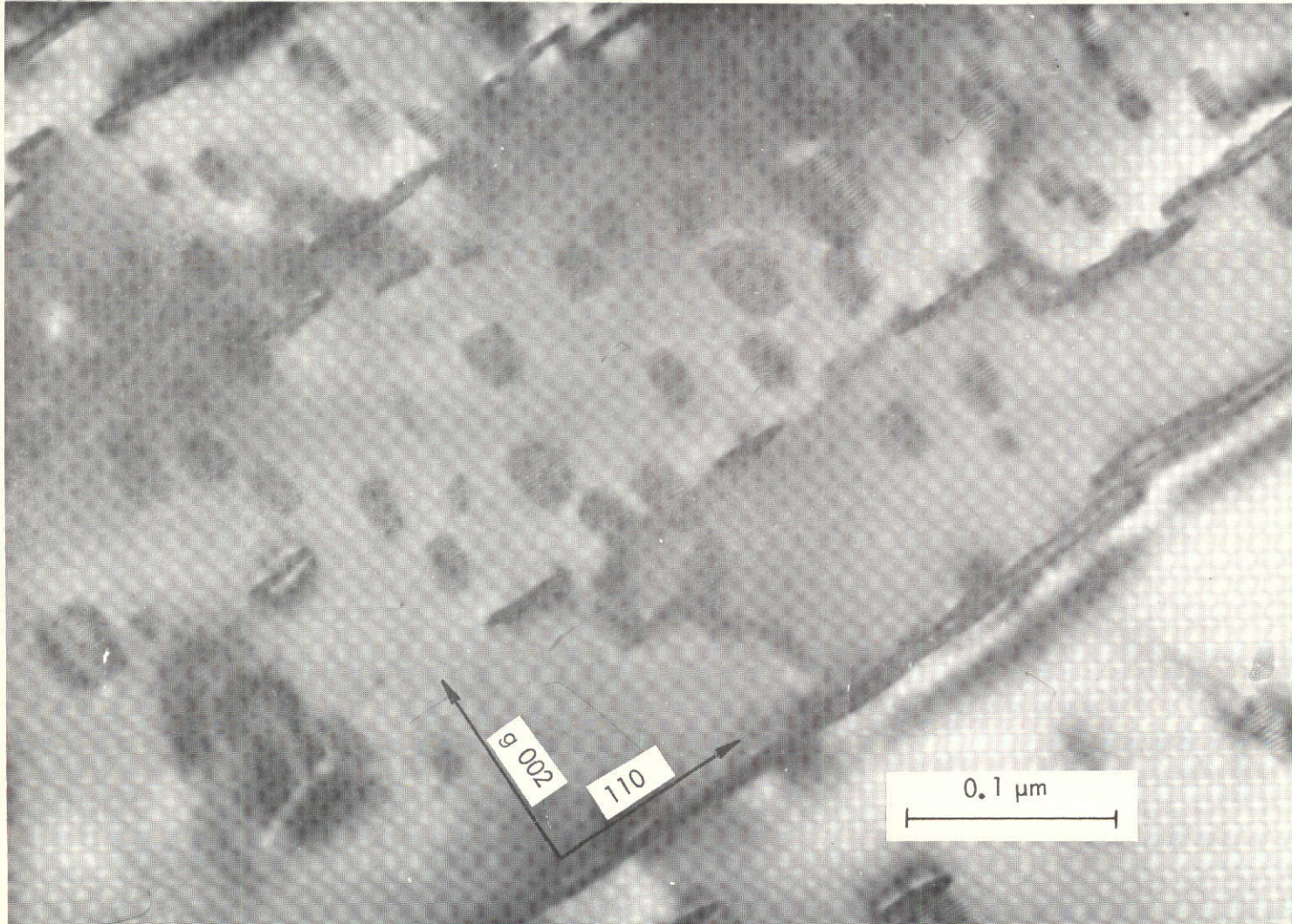


Figure 17. TaC Precipitation in the Cr-0.50TaC Alloy Solution Annealed then Aged 3 Hours at 1422°K (2100°F) (110) Foil Orientation

Table 7. The Air Oxidation Behavior of Selected Alloys at 1422°K (2100°F)

Analyzed Composition a/o	Parabolic Rate Constant* mgs/cm ² -hr ^{1/2}
Cr-.56Ta-.57C-.01Y	0.93
Cr-.78Ta-.77C-.03Y	1.22, 1.62
Cr-1.02Ta-1.14C-.17Y	1.64, 1.90, 2.06
Cr-.54Ta-.49B-.12Y	0.20, 0.49
Cr-1.06Ta-.99B-.11Y	0.43, 0.69

* Values of individual tests reported.

the $\sim 0.5 \pm 0.2 \text{ mg/cm}^2\text{-hr}^{1/2}$ rate constant characteristic of the TaB strengthened compositions is much lower than that observed for material containing TaC. This difference in oxidation behavior must be related to the individual effects that carbon and boron have on oxygen diffusion through the oxide scale.

4.2 INFLUENCE OF THERMOMECHANICAL PROCESSING ON THE PROPERTIES OF Cr-.50Ta(C, B)

The objective of this project was to determine how variations in thermomechanical processing would influence low temperature ductility and high temperature strength of the Cr-.50Ta(C, B) alloy. It involved converting ingot material to test rod using the techniques of extrusion and swaging but incorporating different fabrication and annealing temperatures. Thermal conditions were chosen to yield worked and recovered microstructures presumed most beneficial to low temperature ductility. Three thermomechanical procedures were examined. Choice of the Cr-.50Ta(C, B) alloy for use on the study was based upon its outstanding high temperature strength.

4.2.1 Fabrication

An outline describing the thermomechanical processing study is shown in Figure 18. Test material was processed from two ingots numbered 26 and 27. The results of chemical analyses for major alloying elements and impurity levels in this material are given in Table 1. One half of one ingot (26A in the diagram) was extruded at the solution annealing temperature, 1811°K (2800°F). Final processing involved aging and swaging treatments at 1422°K (2100°F). The other ingot half (26B) was solution treated then aged and fabricated at 1422°K (2100°F). The remaining entire ingot (27) was solution treated then aged and fabricated at 1255°K (1800°F). The reductions taken by extrusion and swaging were kept constant on all three procedures; 85% by extrusion, 75% by swaging.

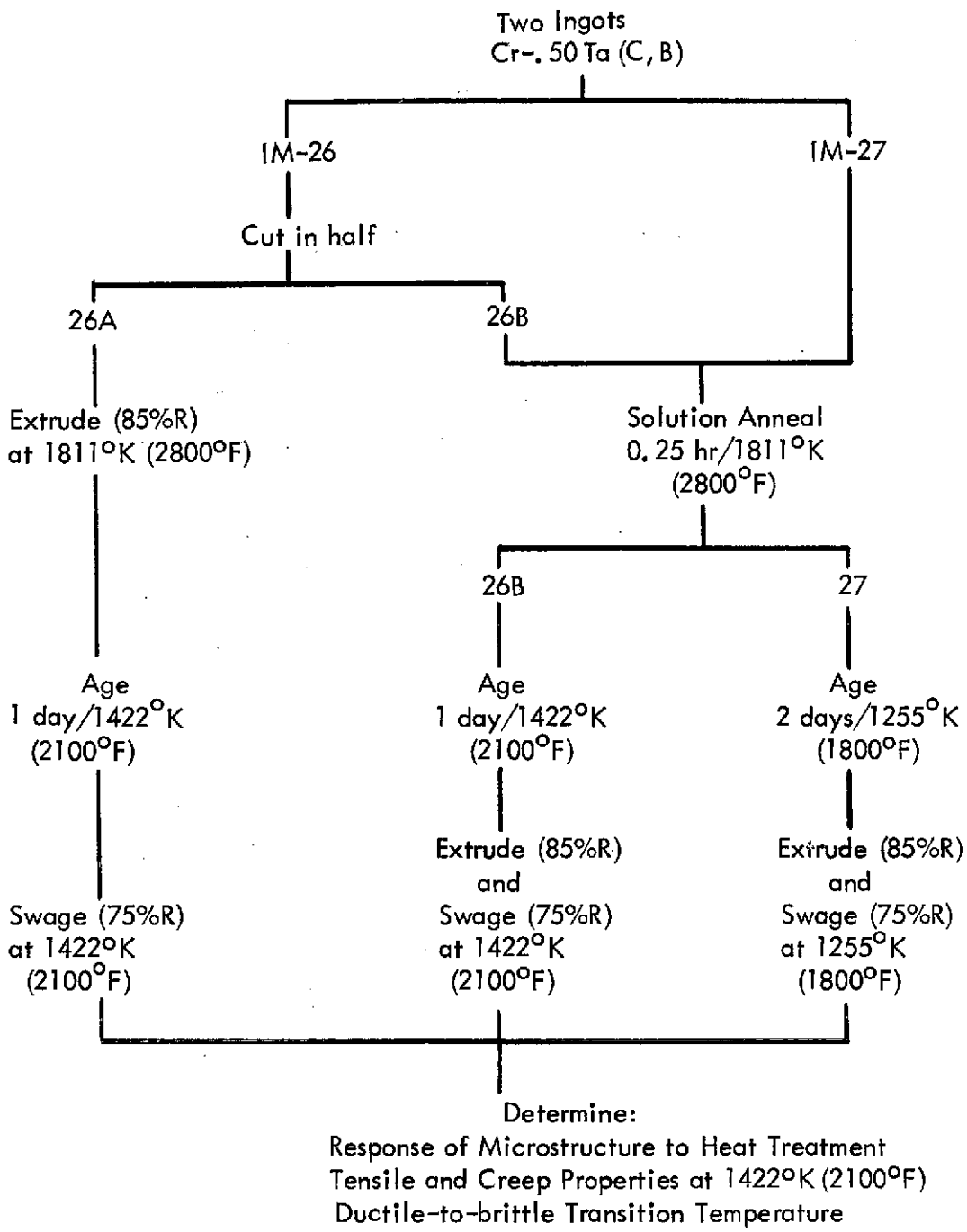


Figure 18. An Outline of the Thermomechanical Processing Study

Piece 26A was severely cracked during fabrication. Cracks following grain boundaries were initially uncovered in this material after extrusion. The condition is exemplified in Figure 19. Extrusion at 1811°K (2800°F), the solution annealing temperature, produced a hot worked microstructure of recrystallized grains containing a grain boundary phase. This microstructure is identical to that which can be developed by solution treatment alone; refer to Figure 2. The grain boundary phase probably consists of Cr_{23}C_6 and Cr_4B or some $\text{Cr}_4(\text{C},\text{B})$ compound. Grain boundary weakness could be a characteristic of this microstructure.

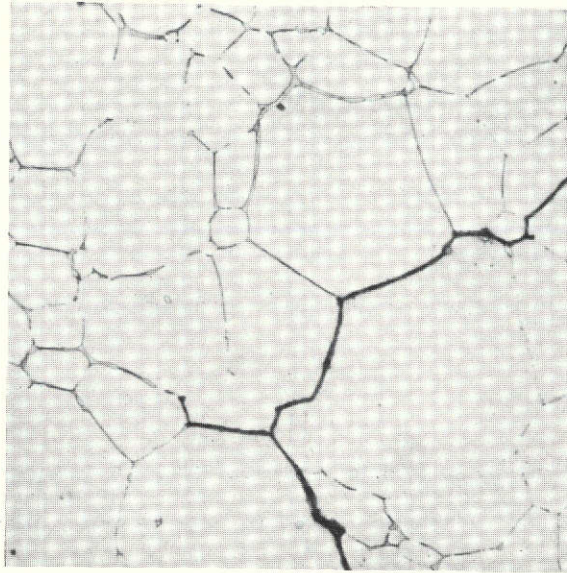
Piece 26A was canned in a heavy wall molybdenum tube prior to extruding at 1811°K (2800°F). Because the thermal expansion coefficient of molybdenum is lower than that of chromium, severe tensile stresses could develop in the chromium bar as it cools from the extrusion temperature*. Stresses produced in this manner and weak grain boundary regions may have combined to cause cracking.

Pieces 26B and 27 were fabricated to test rod without encountering cracking problems. The temperatures at which they were processed permitted use of low carbon steel for canning. Steel has a higher thermal expansion coefficient than does chromium so compressive stresses are produced in the latter upon cooling from fabrication temperatures.

4.2.2 Optical Microstructure

Samples of the three differently fabricated Cr-.50Ta(C,B) pieces were annealed for one hour at temperatures ranging from 1477 to 1811°K (2200 to 2800°F) to study changes of optical microstructure and hardness. Although piece 26A was severely cracked, a sufficient number of small sound coupons were obtained from it permitting this type of study. Crack-free specimens for mechanical property evaluations, however, were not obtained from piece 26A. A summary of the influence of heat treatment on microstructure and hardness is given in Figure 20.

* Extrusion produces a chromium bar encased in and tightly bonded to the canning material.



500X

Figure 19. The Microstructure of Piece 26A in the As-extruded Condition. Extrusion at 1811°K (2800°F) produced a hot worked fully recrystallized microstructure containing a grain boundary phase. Numerous grain boundary cracks were found in this material.

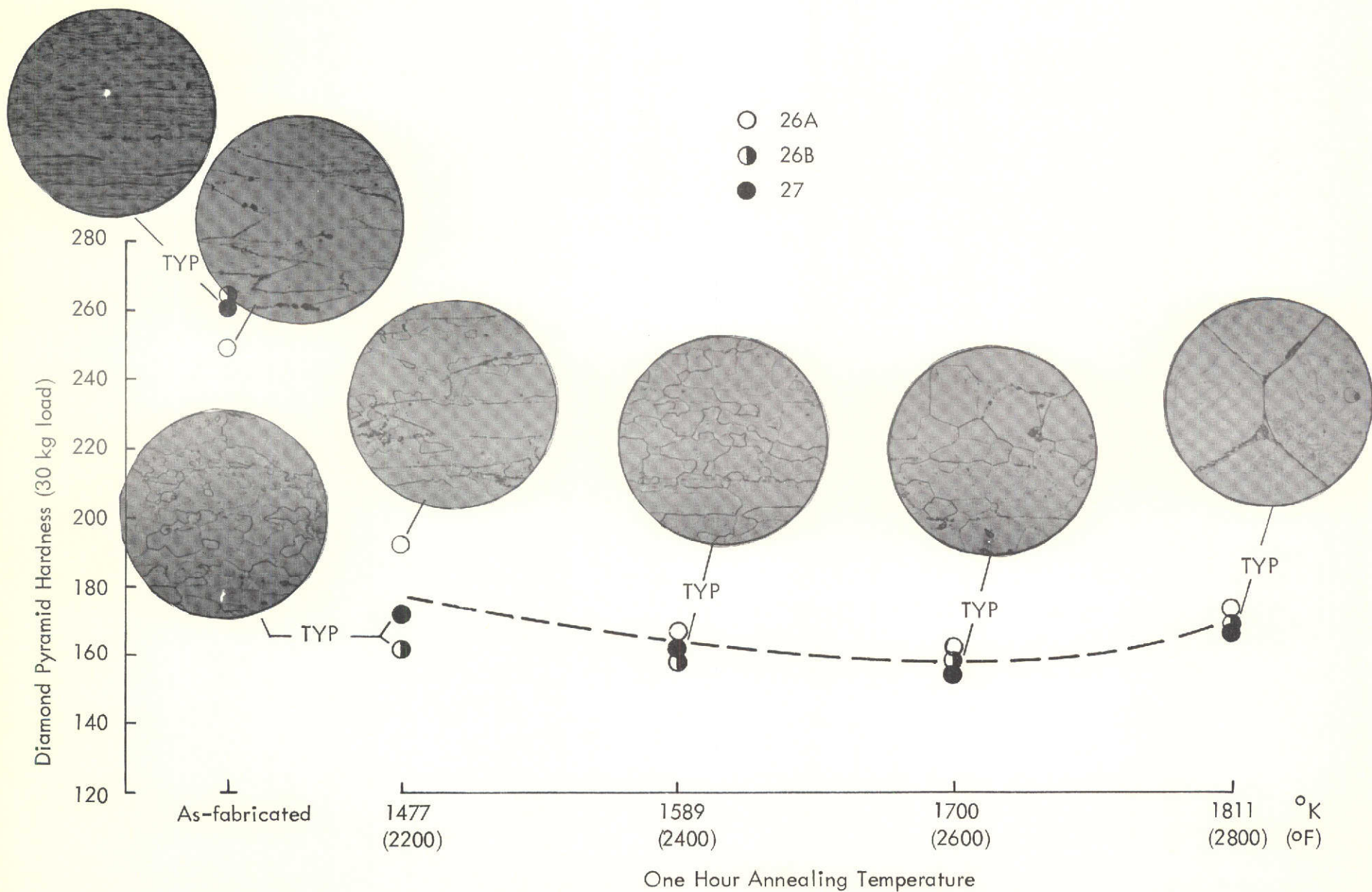


Figure 20. The Influence of Heat Treatment on Microstructure and Hardness of the Cr-.50Ta (C,B) Alloy Fabricated by Three Different Processes. Refer to Figure 18 for fabrication histories. Longitudinal microstructures presented at 250X.

The as-fabricated materials ranged in hardness from approximately 250 to 260 DPH. In this condition, the hardness of piece 26A was lowest, undoubtedly a consequence of the very high extrusion temperature used in its fabrication (see Figure 18). The microstructure of this material consisted of distinct grains somewhat elongated by fabrication. By comparison, a more heavily worked microstructure lacking any grain boundary definition characterized pieces 26B and 27.

A one hour anneal at 1477°K (2200°F) caused partial recrystallization in piece 26A revealed by small equiaxed grain formation and a hardness decrease to 190 DPH. Pieces 26B and 27 were completely recrystallized by similar heat treatment and somewhat lower in hardness. Annealing at temperatures of 1589°K (2400°F) and higher erased any influence of prior fabrication histories, and the three differently processed pieces displayed similar hardness and microstructural characteristics.

4.2.3 Tensile and Creep Properties at 1422°K (2100°F)

Tensile and creep data are presented in Table 8. Ultimate strengths of 394 and 459 MN/m^2 (56.7 and 66.1 ksi) were measured, respectively, on pieces 26B and 27. These results probably reflect the difference in fabrication temperature used to produce the pieces. Piece 26B was fabricated at 1422°K (2100°F); piece 27 was fabricated at 1255°K (1800°F).

Creep tests were run on the as-fabricated pieces at 104 MN/m^2 (15 ksi), and similar results were observed. Although the tensile strengths of both pieces were approximately four times higher than the creep test stress, failure occurred in only 20 hours. This may be related to gross microstructural instability of the worked and recovered conditions. The data shown in Figure 20 relating annealing temperature to hardness and microstructure does indicate that the wrought materials would probably undergo complete recrystallization in a few hours at the test temperature of 1422°K (2100°F).

Table 8. The Influence of Fabrication History on Tensile and Creep Properties of the Cr-.50Ta(C, B) Alloy Measured at 1422°K (2100°F)*

(a) Tensile Properties

Piece No.	0.2% Yield		U. T. S.		El. (%)	Area Red. (%)
	MN/m ²	(ksi)	MN/m ²	(ksi)		
26B As-fabricated	374	53.8	394	56.7	17.0	65.5
27 As-fabricated	448	64.7	459	66.1	13.0	64.1

(b) Creep Properties

Piece No.	Test Stress		Min. Creep Rate	Rupture Life	Rupture Ductility	
	MN/m ²	(ksi)	%/Hr.	Hrs.	% El.	% R. A.
26B As-fabricated	104	15.0	0.4	19.2	36.0	75.7
27 As-fabricated	104	15.0	0.4	21.0	38.0	79.5
26B Soln. Ann. plus Aged**	194	28.0	0.013	112.3	13.0	66.6
	208	30.0	0.018	100.5	11.0	61.6

* Refer to Figure 18 for fabrication histories. Piece 26A was too severely cracked to permit evaluation.

**0.25 hr/1811°K (2800°F) + 3 hr/1422°K (2100°F) heat treatment.

Two creep tests were run on specimens of piece 26B given a solution anneal and aging heat treatment. Data were gathered at stress levels approximately twice that at which as-fabricated material was tested. Furthermore, the test stresses employed represent roughly 80% of the ultimate strength displayed by the Cr-.50Ta(C, B) alloy in the solution treated and aged condition*. Even under these extreme stress conditions, the heat treated specimens displayed over an order of magnitude lower creep rate and a five times longer rupture life compared to material tested as-fabricated.

4.2.4 Ductile-to-Brittle Transition Behavior

Specimens from pieces 26B and 27 were tensile tested in the as-fabricated condition to determine the temperatures at which transition from ductile-to-brittle behavior occurred. Tests were also run on 26B material in the solution annealed and aged condition. These data and values of ductile-to-brittle transition temperatures (DBTT) are presented in Table 9. The DBTT points were estimated from the temperature dependency of reduction of area plots given in Figure 21.

The transition temperature of pieces 26B and 27 were, respectively, 700 and 781°K (800 and 950°F). The slightly lower DBTT of piece 26B might be associated with use of a higher temperature in its fabrication. Regardless, both as-fabricated materials were very brittle in spite of their worked and recovered conditions.

The failure to obtain an improvement in DBTT by fabrication to produce worked and recovered microstructures is further emphasized by the results obtained on solution annealed and aged material. A 644°K (700°F) DBTT was measured on material in this recrystallized extremely coarse grain condition, matching the lowest level of the property displayed by material in the worked and recovered condition.

* Refer to Table 3 for tensile properties of solution annealed and aged material.

Table 9. The Influence of Fabrication History on Low Temperature Tensile Properties of Cr-. 50Ta(C, B)⁽¹⁾

Piece No.	Test °K	Temp. °F	Elongation		Area Red. %	0.2% Yield		U. T. S.		DBTT ⁽³⁾	
			% Uniform	% Total		MN/m ²	ksi	MN/m ²	ksi	°K	°F
26B As-fabricated	532	500	0.0	0.0	0.0	--	--	650	93.5 ⁽⁴⁾	700	800
	644	700	0.0	0.0	0.0	673	97.1	688	98.9 ⁽⁴⁾		
	700	800	1.0	1.0	2.8	696	100.2	715	103.1 ⁽⁴⁾		
	755	900	2.6	10.1	44.2	670	96.7	700	100.9		
27 As-fabricated	532	500	0.0	0.0	0.0	--	--	672	96.7 ⁽⁴⁾	781	950
	644	700	0.0	0.0	0.0	--	--	698	100.3 ⁽⁴⁾		
	755	900	1.0	1.0	1.9	724	104.1	741	106.6 ⁽⁴⁾		
	866	1100	1.9	8.0	33.1	701	101.1	731	105.5		
26B Sol'n annealed + aged ⁽²⁾	644	700	5.0	5.0	5.2	220	31.7	380	54.8 ⁽⁴⁾	644	700
	700	800	11.0	11.0	13.8	224	32.3	378	54.6 ⁽⁴⁾		
	755	900	8.6	16.0	39.0	222	32.1	367	53.0		

(1) Refer to Figure 18 for fabrication histories. Piece 26A was too severely cracked to permit evaluation.

(2) 0.25 hr/1811°K (2800°F) + 3 hr/1422°K (2100°F) heat treatment.

(3) The approximate temperature at which % reduction of area equals 5%. (Figure 21)

(4) Specimen fractured before reaching the true ultimate strength.

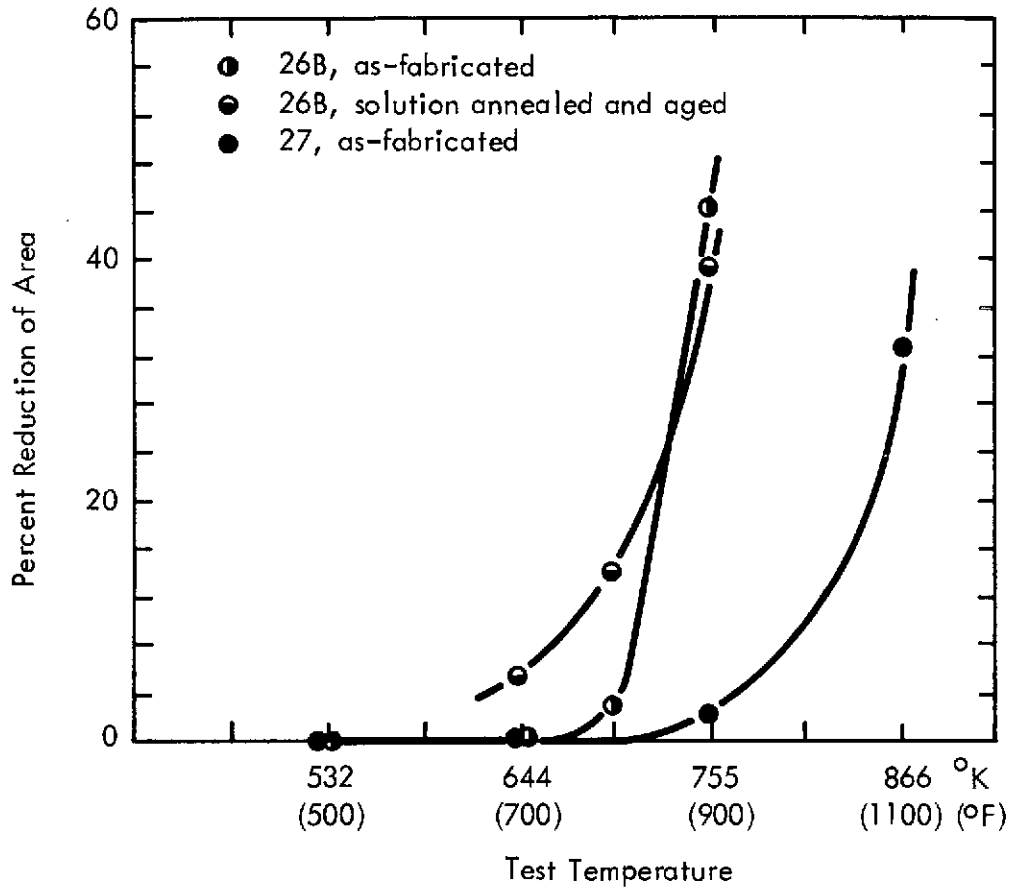


Figure 21. The Influence of Fabrication History on the Ductile-to-Brittle Transition Behavior of Cr-.50Ta(C, B)

4.3 SOLUBILITY OF CARBON AND BORON IN CHROMIUM

The temperature dependency of carbon and boron solubility in chromium was examined on a project run concurrently with the alloy development and thermomechanical processing studies previously reported. Samples of chromium alloyed with 0.50, 0.75, and 1.00 a/o carbon or boron were heat treated at temperatures ranging from 1589 to 1866°K (2400 to 2900°F), then examined metallographically to define the temperature dependency of grain size. Solvus temperatures were assumed to be indicated by a sharp increase in grain size. Details of the techniques used to melt, fabricate, and evaluate material on this study are given in the Materials and Experimental Procedures section.

4.3.1 Chemical Analyses

The results of chemical analyses for alloying and common impurity elements in the heats prepared for the solubility study are presented in Table 10. Nominal compositions were closely approached in each case, and oxygen and nitrogen levels in the two heats examined were maintained one or two orders of magnitude below that of the major alloying elements. The Cr-C heats were melted successively in a single furnace load as were the Cr-B heats. Analyses for oxygen and nitrogen in only one alloy of each type, therefore, was sufficient to characterize contamination for the six study compositions.

4.3.2 Solubility Data

The solubility study results are summarized in Figure 22 where grain size is plotted as a function of annealing temperature for the Cr-C and Cr-B compositions. Solvus temperatures in the ranges 1755 to 1785°K (2700 to 2750°F) for 0.5 a/o carbon, and 1805 to 1822°K (2790 to 2820°F) for 0.75 a/o carbon are indicated by the pronounced increases in grain size. Microstructures formed in the Cr-0.75C composition by annealing at 1589, 1700, and 1822°K (2400, 2600, and 2820°F), are presented in Figure 23. They are also representative of the conditions developed in the Cr-.50C alloy by similar heat treatment. Indications of minor liquation were

Table 10. Chemical Analyses of the Solubility Study Alloys

Nominal Composition (a/o)	Analytical Results, a/o			
	Carbon	Boron	Oxygen	Nitrogen
Cr-0.50C	0.46	-	-	-
Cr-0.75C	0.80	-	0.021	<0.007
Cr-1.00C	1.12	-	-	-
Cr-0.50B	-	0.48	-	-
Cr-0.75B	-	0.77	0.003	<0.007
Cr-1.00B	-	0.91	-	-

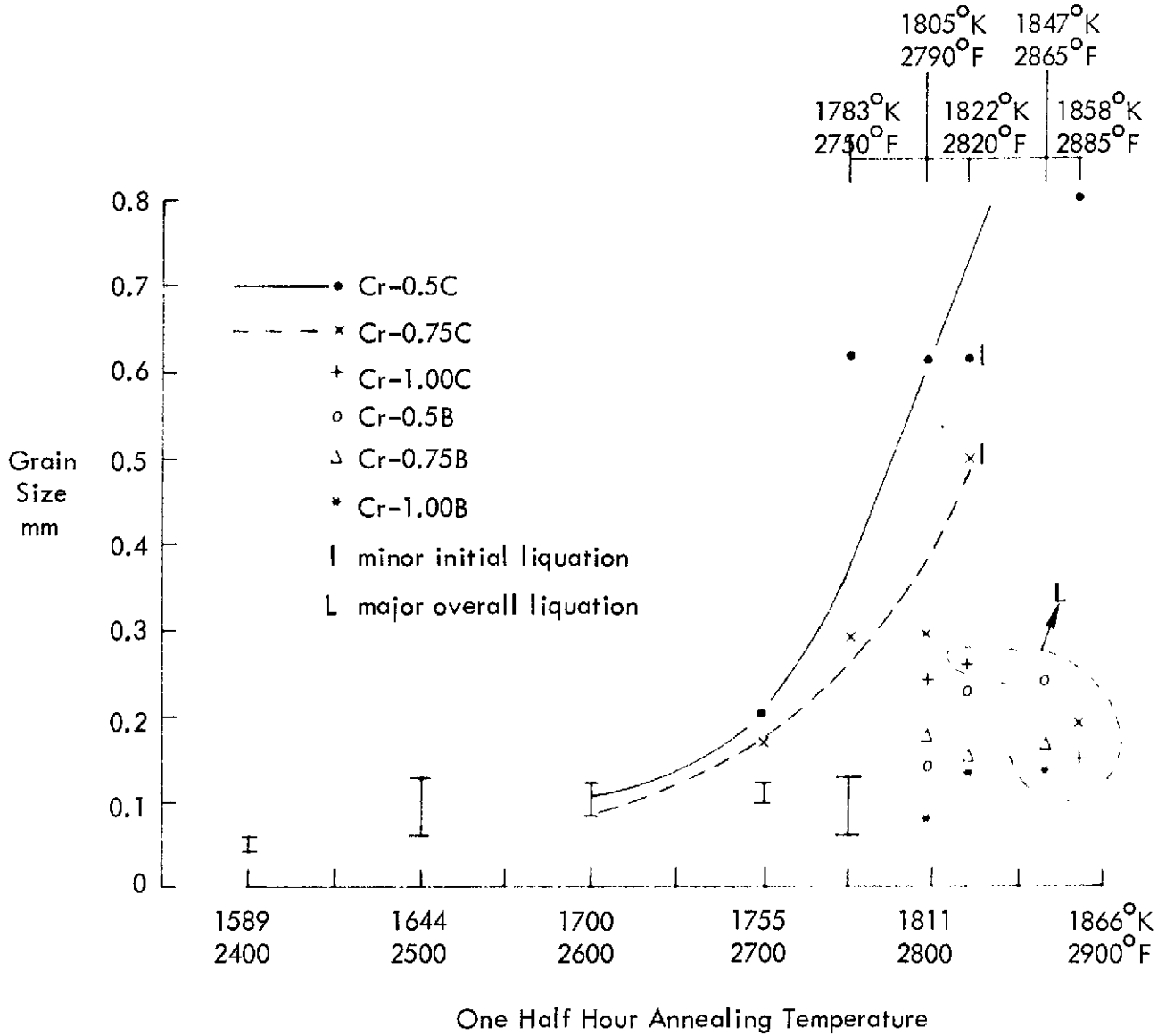
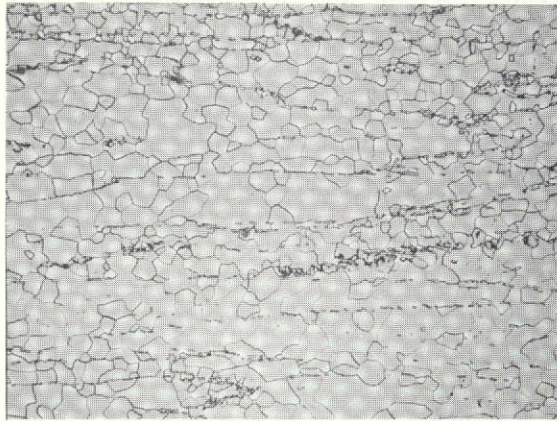
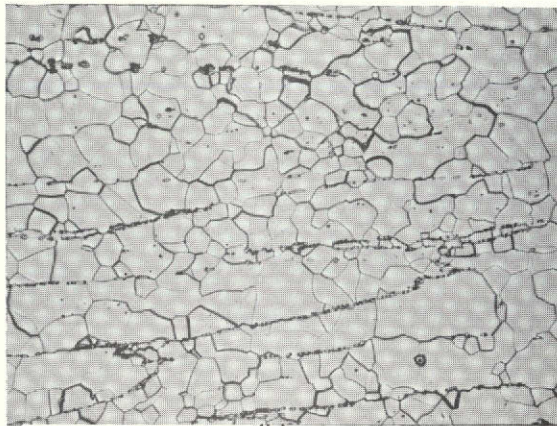


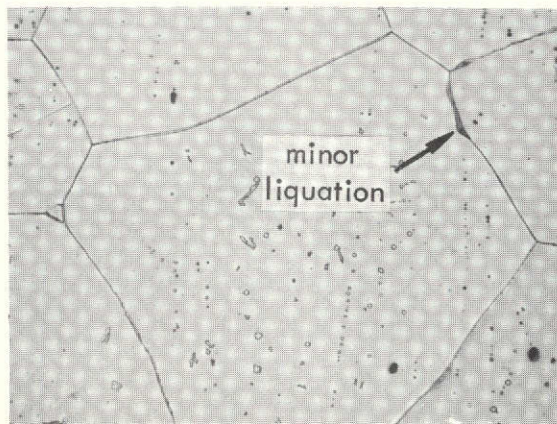
Figure 22. The Influence of Heat Treatment on Grain Size of the Cr-C and Cr-B Compositions



(a)



(b)



(c)

Figure 23. Microstructural Response of the Cr-0.75C Composition to Heat Treatment 60X
(a) 1589°K (2400°F) (b) 1700°K (2600°F) (c) 1822°K (2820°F)

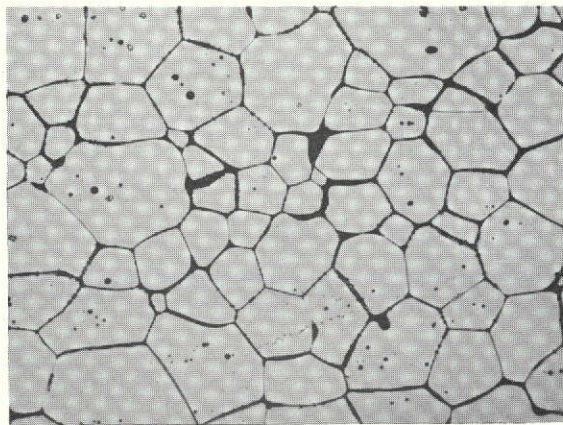
noted in the coarse grain microstructure caused by annealing at 1822°K (2820°F), suggesting that the Cr-Cr₂₃C₆ eutectic lies below this temperature and was crossed prior to complete solutioning of the Cr₂₃C₆ phase.

An abrupt increase in grain size was not noted in the Cr-1.0C alloy heat treated up to 1805°K (2790°F). At a slightly higher temperature, 1822°K (2820°F), the composition displayed evidence of overall gross liquation indicating the Cr-Cr₂₃C₆ eutectic temperature lies between 1805 and 1822°K (2790 and 2820°F), and the maximum solubility of carbon in chromium is below 1 a/o. The microstructure formed in the Cr-1.0 a/o C alloy by annealing at 2820°F is presented in Figure 24. This behavior, in conjunction with the previously discussed results, suggests that the maximum amount of carbon soluble in chromium lies between 0.75 and 1.0 a/o.

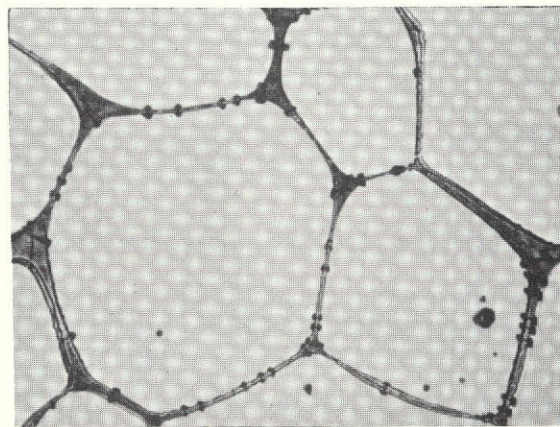
Evidence of overall liquation, similar to that noted in the Cr-1.0 a/o C composition after annealing at 1822°K (2820°F), was found in the 0.75 a/o C alloy after 1858°K (2885°F) heat treatment indicating the solidus is exceeded by this composition-temperature condition. On the other hand, the coarse grain structure formed in the 0.5 a/o C alloy by annealing at 1858°K (2885°F) is evidence that the composition-temperature condition falls within the bounds of the solidus.

Heat treatment up to 1822°K (2820°F) failed to abruptly coarsen the grain structure of the three Cr-B compositions, and each displayed evidence of major liquation upon annealing at 1847°K (2865°F). The microstructures developed in the Cr-0.5B alloy by 1700, 1822, and 1847°K (2600 , 2820 , and 2865°F) heat treatment are presented in Figure 25. The Cr-Cr₄B eutectic apparently lies between 1822 and 1847°K (2820 and 2865°F), and the maximum amount of boron soluble in chromium appears to be less than 0.5 a/o.

Solvus, solidus, and eutectic lines for the Cr-C and Cr-B systems as interpreted from the solubility study data are plotted in Figures 26 and 27. Structures displaying a 0.3 mm grain

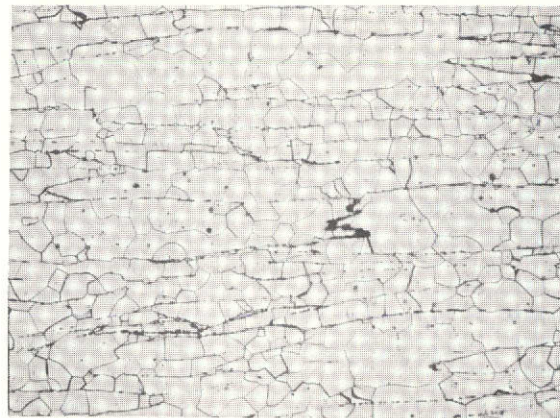


60X

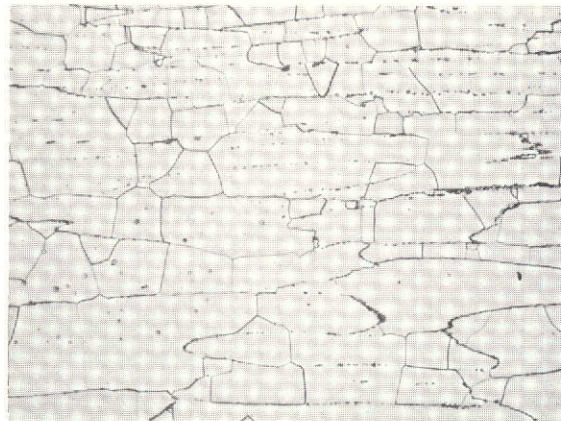


250X

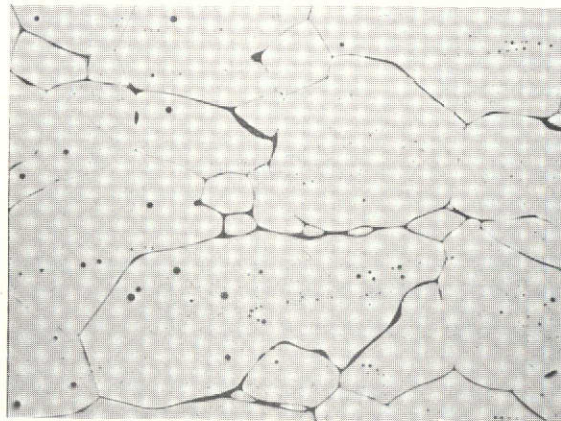
Figure 24. Overall Grain Boundary Liquation Caused in the Cr-1.0C Composition by Heat Treatment at 1822°K (2820°F)



(a)



(b)



(c)

Figure 25. Microstructural Response of the Cr-0.5B Composition to Heat Treatment 60X
(a) 1700°K (2600°F) (b) 1822°K (2820°F) (c) 1847°K (2865°F)

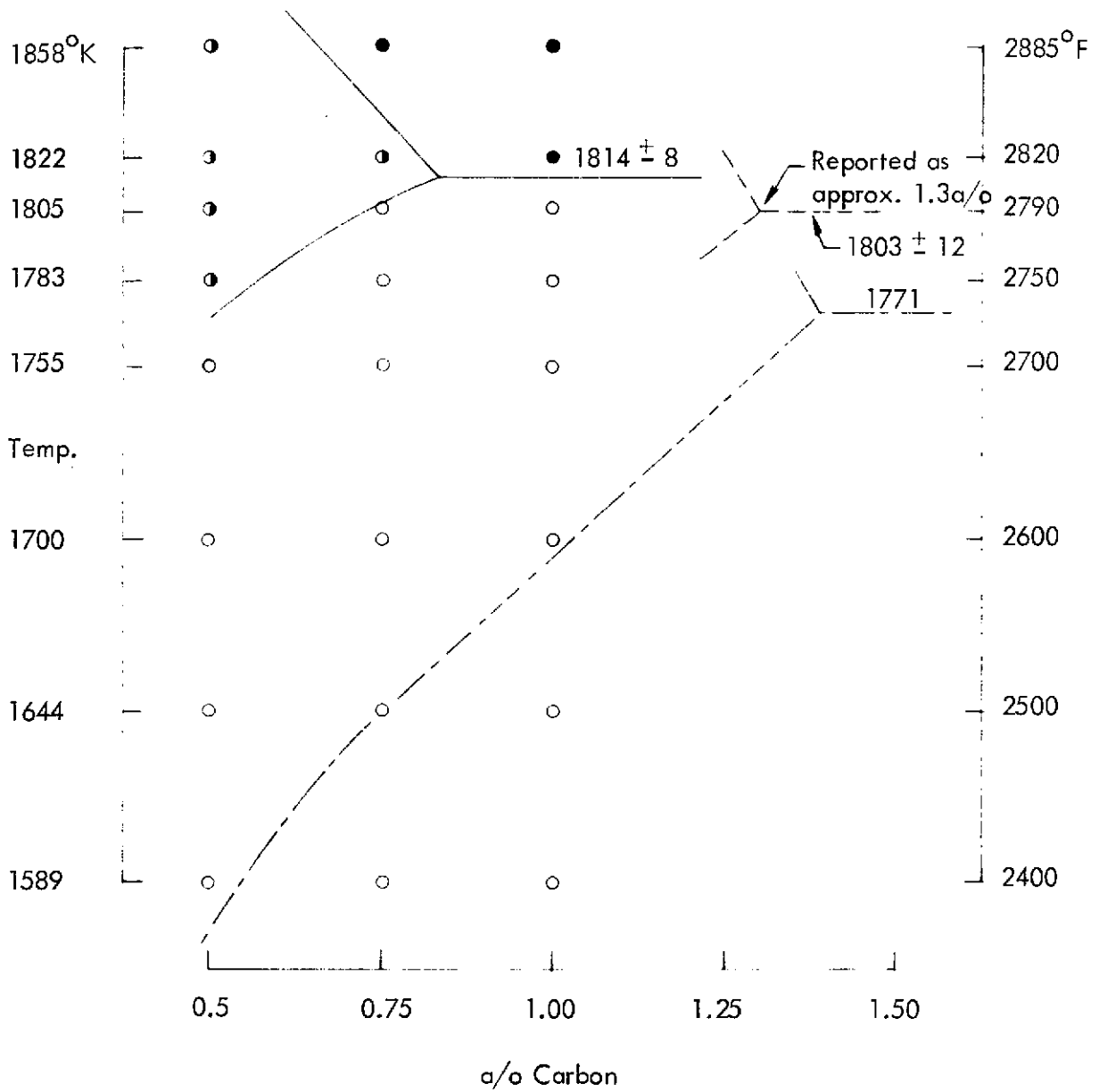
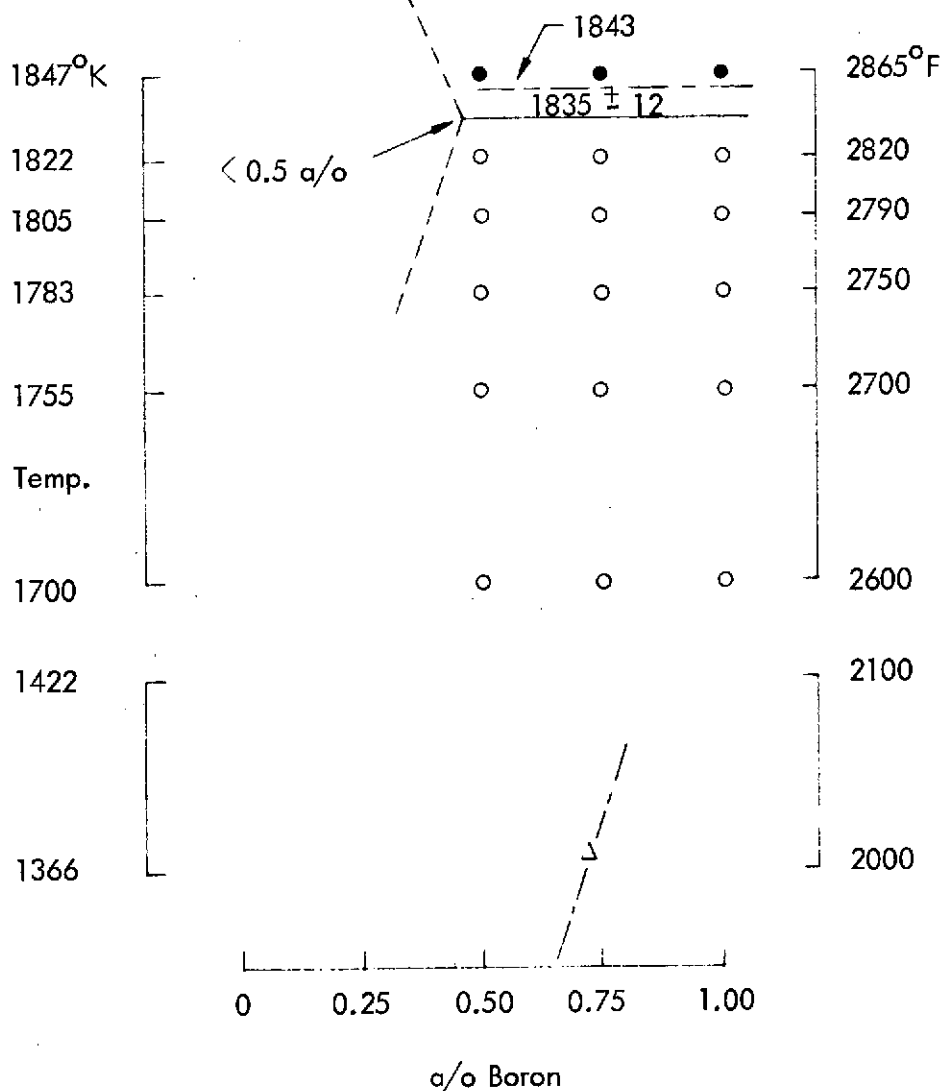


Figure 26. Terminal Solubility and Melting in the Cr-C System



- Liquation
 - Fine grain microstructure
- (Present
Study)

--- T. F. Fedorov et. al, Soviet Powder Met, 1962, Vol. 6, p. 435

F. I. Shamrai, T. F. Fedorov, Issledovanya Metallov Zhidhom i Tverdom Sostoyaniyakh, p. 255, Izd. Nauka, Moscow, 1964

(F. A. Shunk, Constitution of Binary Alloys, 2nd Supplement, McGraw-Hill, 1969)

Figure 27. Terminal Solubility and Melting in the Cr-B System

size or less after annealing were assumed to indicate that complete solutioning was not achieved and are presented as fine grain microstructure points. Grain sizes of 0.5 mm and larger were assumed indicative of complete solutioning and are presented as coarse grain microstructure points. The limited information published on the Cr-C and Cr-B systems are included on the respective diagrams. The Cr-Cr₂₃C₆ and Cr-Cr₄B eutectic temperatures derived from this investigation are in good agreement with the most recently published information. The observed solubility of carbon and boron in chromium, however, is appreciably less than indicated by other work.

4.4 IDENTIFICATION OF BORIDES FORMED IN Cr-Ta-B AND Cr-Cb-B ALLOYS

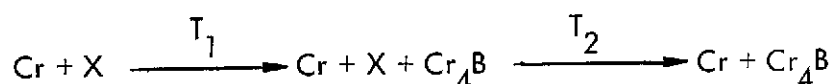
A successful effort was made to identify the crystal structures and formulas of the complex boride strengthening phases formed in Cr-Ta-B and Cr-Cb-B alloys. Previous work had shown that these compounds were not the simple MB or MB₂ types anticipated to be stable in the alloys. Background information on this subject is presented below.

4.4.1 Previously Reported Data

An extensive study of elevated temperature boride formation and stability in several Cr-Ta-B and Cr-Cb-B alloys was previously undertaken^(5,6). Samples of the alloys were heat treated at temperatures ranging from 1422 to 1755°K (2100 to 2700°F), rapidly quenched, then dissolved to release any boride compounds. These were examined by x-ray diffraction and fluorescent analysis for identification.

A complex tantalum-rich boride formed in the Cr-Ta-B alloys. Its diffraction pattern could not be indexed nor did it match that of any cataloged compound, consequently, the boride was referred to as X phase. A columbium-rich boride of similar diffraction characteristics was also observed to form in the Cr-Cb-B alloys.

A transition from stability of these X phases to that of Cr_4B occurred at high temperatures, and alloying level influenced the transition temperature range. Increasing the alloying metal-to-boron ratio increased the temperature to which the X phases were stable. A review of elevated temperature boride stability observed for the alloys studied is given below.



Composition a/o	T_1		T_2	
	$^{\circ}\text{K}$	$(^{\circ}\text{F})$	$^{\circ}\text{K}$	$(^{\circ}\text{F})$
Cr-.5Cb-.5B	< 1422	(< 2100)	~1700	(~2600)
Cr-.5Cb-.25B	~1700	(~2600)	> 1755	(> 2700)
Cr-.5Ta-.5B	< 1422	(< 2100)	> 1755	(> 2700)
Cr-.5Ta-.25B	~1700	(~2600)	> 1755	(> 2700)

Debye x-ray diffraction patterns of both the tantalum-rich and columbium-rich X phase borides are displayed in Figure 28. Also shown in the figure are the patterns obtained for a mixture of X phase and Cr_4B and Cr_4B alone. The tantalum-rich and columbium-rich X phases obviously have the same crystal structure as judged from the similarity of their diffraction patterns. However, significant differences in line position in the back reflection region of the patterns ($\theta > 45^{\circ}$) indicates a slight difference in lattice parameter values exists.

4.4.2 Current Program

The unknown tantalum-rich and columbium-rich boride diffraction patterns were successfully indexed on this program and linked to compounds of the M_3B_2 type. Diffraction data for the tantalum-rich compound are presented in Part (a) of Table 11 and indexed as tetragonal, $a = 5.905 \times 10^{-10} \text{ m}$ (5.905 \AA), $c = 3.231 \times 10^{-10} \text{ m}$ (3.231 \AA). Presented in Part (b) of Table 11 are data reported by Beattie⁽¹⁰⁾ for an analogous parameter tetragonal mixed metal boride of $(\text{M}, \text{M}')_3\text{B}_2$ type ($\text{M} = \text{Mo} + \text{Al} + \text{Ti}$, $\text{M}' = \text{Cr} + \text{Fe} + \text{Ni}$, $\text{M}/\text{M}' \sim 2$). The

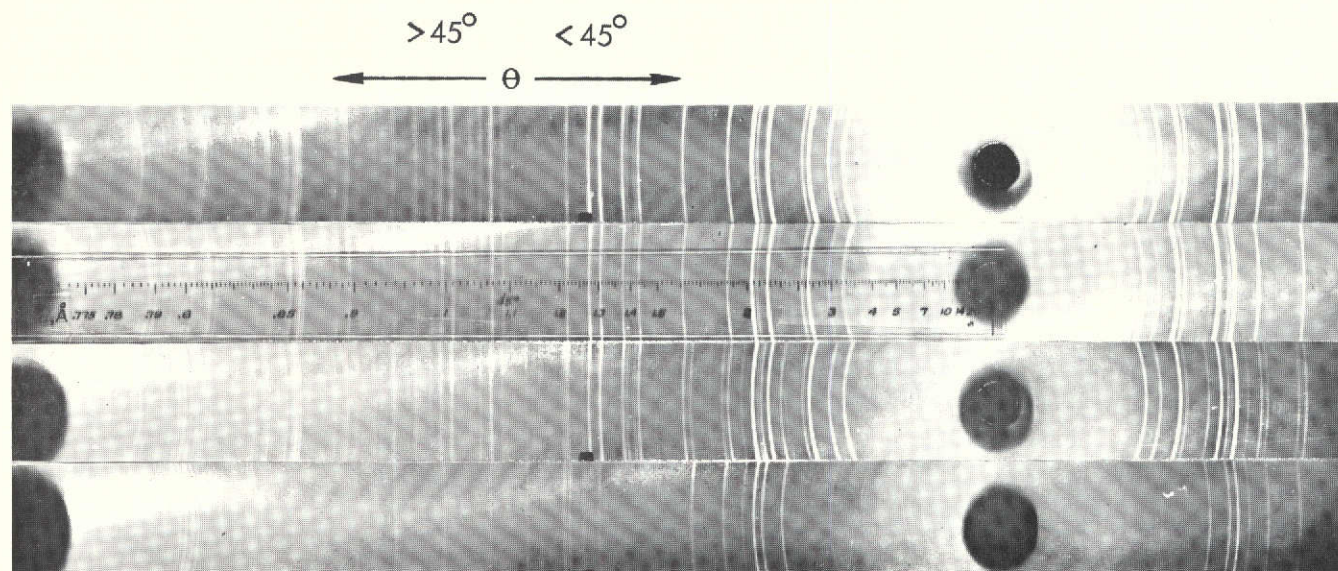


Figure 28. Diffraction Patterns of Boride Phases Extracted from Tantalum and Columbium Boride Strengthened Chromium-base Alloys. Top-to-bottom: 1. Tantalum-rich X phase boride; 2. Columbium-rich X phase boride; 3. Tantalum rich X phase boride plus Cr_4B ; 4. Cr_4B

Table 11. Indexed Diffraction Data for the Tantalum-rich X Phase Boride (part a),
and That Reported for a Mixed Metal Boride of M_3B_2 Type (part b)

(a)			(b) Ref. 10		
d spacing $m \times 10^{10}$	hkl*	Intensity** I/I_1	d spacing* $m \times 10^{10}$	hkl**	Intensity*** I/I_1
3.2306	001	60	3.14	001	31
2.9525	020	40	2.89	020	10
2.6389	120	90	2.586	120	81
2.5544	111	25	2.490	111	42
2.1784	021	95	2.124	021	100
2.0867	220	35	2.043	220	20
2.0437	121	100	1.994	121	100
1.8675	130	40	1.828	130	39
1.7535	221	10			
1.6385	230	15			
1.6158	131, 002	35	1.564	002	20
1.4607	231	5			
1.4324	140	35	1.403	140	14
1.4171	002	20			
1.3917	330	10	1.364	330	4
1.3791	122	35	1.338	122	19
1.3433	041	10	1.313	041	4
1.3096	141	45	1.277	141	28
1.2784	331	40	1.247	331	20
1.2218	132	20	1.190	132	13

* Tetragonal indexing, $a = 5.905 \text{ \AA}$
 $c = 3.231 \text{ \AA}$
Proposed stoichiometry $(Ta, Cr)_3B_2$,
 $Ta/Cr \sim 2$

** Densitometer measurement.

* $(M, M')_3B_2$ $M = Mo + Ti + Al$,
 $M' = Cr + Fe + Ni$, $M/M' \sim 2$

** Tetragonal indexing, $a = 5.783 \text{ \AA}$
 $c = 3.134 \text{ \AA}$

*** Diffractometer measurement.

similarity of reflecting lattice planes and line intensities of the X phase and $(M, M')_3B_2$ patterns, the equivalence in atomic size of tantalum with the metals Mo, Al, and Ti, and the tantalum-rich character of the X phase all indicate a probably $(Ta, Cr)_3B_2$, Ta/Cr \sim 2, stoichiometry for the unknown compound.

As previously mentioned, the tantalum-rich and columbium-rich X phase boride diffraction patterns were analogous except for a shift in line positions in the back reflection region indicating slightly larger lattice parameters for the latter compound. This was confirmed by actual measurement where the tetragonal parameters $a = 5.925 \times 10^{-10} \text{ m}$ (5.925 \AA) $c = 3.240 \times 10^{-10} \text{ m}$ (3.240 \AA), were determined for the columbium-rich compound. Diffraction data for the compound are presented and indexed in Table 12. It follows from previous discussion that its probably chemical formula is $(Cb, Cr)_3B_2$, Cb/Cr \sim 2.

Table 12. Indexed Diffraction Data for the Columbium-rich X Phase Boride

d spacing $m \times 10^{10}$	hkl*	Intensity** I/I_1
3.2433	001	35
2.9631	020	20
2.6511	120	70
2.5636	111	40
2.1875	021	95
2.0969	220	45
2.0517	121	100
1.8755	130	55
1.7408	221	< 5
1.6439	230	5
1.6208	131, 002	40
1.4383	140	35
1.4231	022	5
1.3980	330	10
1.3838	122	35
1.3487	041	5
1.3264	240	5
1.3148	141	40
1.2833	331, 222	50
1.2264	241, 132	30

* Tetragonal indexing $a = 5.925 \text{ \AA}$, $c = 3.240 \text{ \AA}$
 Probable $(\text{Cb}, \text{Cr})_3\text{B}_2$, Cb/Cr ~ 2

** Densitometer measurement.

5.0 CONCLUSIONS

The following are the principal conclusions drawn from a study of chromium alloys dispersion strengthened by the putative TaC, TaB, CbC, and CbB compounds.

1. TaC and TaB are the most potent strengthening phases.
2. When combined, TaC and TaB can strengthen chromium to a far greater level than obtained by using the individual compounds.
3. The high temperature creep strength of the best available superalloys can be significantly exceeded by dispersion strengthened chromium.
4. The improvement of low temperature ductility remains as a major problem to be solved before the engineering potential of these alloys can be realized.

6.0 REFERENCES

1. O. N. Carlson, L. L. Sherwood, and F. A. Schmidt, *J. Less-Common Metals*, 1964, Vol. 6, pp 439-50.
2. E. P. Abrahamson, N. J. Grant, *Trans. ASM*, 1958, Vol. 50, pp 705-21.
3. J. W. Clark, General Electric Co., NASA CR-92619, June 30, 1967.
4. N. E. Ryan, *J. Less-Common Metals*, Vol. 2, 1966, pp. 221-48.
5. A. M. Filippi, *Met. Trans.*, 1972, Vol. 3, pp 1727-33.
6. A. M. Filippi, Westinghouse Electric Corp., NASA CR-72883, November 26, 1970.
7. A. M. Filippi, Westinghouse Electric Corp., NASA CR-72727, December 22, 1968.
8. A. M. Filippi, *J. Less-Common Metals*, Vol. 30, 1973, pp 153-158.
9. O. D. Sherby, *Acta Met.*, Vol. 10, 1962, pp 135-147.
10. H. J. Beattie, Jr., *Acta Cryst.*, Vol. 11, 1958, p. 607.